Title
An essential role for H3K4 methyltransferase KMT2D in heart development

Author
Ang, Siang Yun

Publication Date
2015

Peer reviewed|Thesis/dissertation

An essential role for H3K4 methyltransferase KMT2D in heart development

by

Siang Yun Ang

DISSERTATION

Submitted in partial satisfaction of the requirements for the degree of

DOCTOR OF PHILOSOPHY

in

Biomedical Sciences

in the

GRADUATE DIVISION

of the

UNIVERSITY OF CALIFORNIA, SAN FRANCISCO

Approved:

[redacted]

If I have seen further,

it is by standing on the shoulders of giants.

- Sir Isaac Newton

To the great scientists I have met along the way,

for your mentorship and guidance.

And to my family and Joe,

for your constant support and inspiration

throughout my scientific journey.

Acknowledgements

This work is the culmination of an interesting and enriching research experience. There were many technical hurdles, which I did not anticipate when I first started out, but I have benefited from the experience of many scientific mentors and colleagues who were willing to lend a helping hand. Personally, I have been deeply motivated to improve the understanding of Kabuki Syndrome and congenital heart disease, and I still wish I could do more. Nonetheless, I am sure future research will further illuminate these fields, and I am glad to have been part of them.

I would like to express my deepest appreciation for my graduate advisor, Dr. Benoit Bruneau. He first ignited my excitement in this project, and his infectious enthusiasm for science has been inspiring. Benoit has given me freedom and resources to explore different directions of my work, which has been invaluable in helping me grow as an independent scientist.

I would also like to thank my thesis committee members, who have been immeasurably supportive during my PhD studies. Dr. Takashi Mikawa, my committee chair, has taught me to be unafraid of asking the big questions and pursuing their answers. Dr. Deepak Srivastava has provided great constructive input on cardiac biology, and Dr. Daniel Lim's expertise on histone

methyltransferases has been enlightening during our discussions. Together, their insights have been key to focusing and improving the work in this dissertation.

I am also very grateful for the Bruneau lab members, who have been incredibly helpful and generous in sharing their ideas and time with me. Paul Delgado, Joshua Wythe and Patrick Devine have been wonderful mentors in teaching me many basic techniques and concepts in molecular biology and mouse work. Luis Luna-Zurita and Elphège Nora have given me practical scientific advice and provided amazing company during late nights in the lab. Alec Uebersohn, Dario Miguel-Perez, John Wylie, and Daniel He have been crucial in providing their technical expertise for experiments presented in this work. I had really useful discussions with Swetansu Hota and Irfan Kathiriya, and sharing graduate school experiences with Jeffrey Alexander, Shan-Shan Zhang and Matthew George has been great. I have been very lucky to have such terrific collegial labmates, and they have definitely made it a pleasure to be part of the Bruneau lab. I would also like to thank the staff members of the Gladstone cores, including the Bioinformatics Core, the Genomics Core, the Stem Cell Core and the Histology Core for helping me with technical aspects of my project.

Outside of the lab, the unwavering support of my family and friends has been indispensable. My family has always been very encouraging of my decisions, and it has been an interesting challenge explaining my work to them in Mandarin Chinese. NASBS and VJC friends – particularly Weixin, Yn Ay, Chun and Siew

Sze - have always been there for me. My fellow Wisconsin-ites, Terence and Alan, have also helped to keep me grounded. Ivana has always put a smile on my face, even from afar in Boston. I am fortunate to have these friends who reach out to me, despite being in different continents and time zones.

I also couldn't have managed this journey without the Singaporean community in UCSF, or what I affectionately term the "Underground Singaporean Network". When I ventured into unfamiliar experiments or needed advice on troubleshooting, they have been a tremendous help with their experiences in different research fields and labs. More importantly, we have shared great adventures together during our time in San Francisco. Sarah and Brenda have been the best housemates, and our dinner conversations has made for many enjoyable evenings and weekends. Fong, Jasmine and Jiamin have been part of many wacky shenanigans, and my time here would not have been the same without them. Jean, my fellow foodie and diving buddy, has also been an essential part of my life in San Francisco.

I would also like to thank the tireless staff that manages the Biomedical Sciences graduate program, including Lisa Magargal, Monique Piazza, Nathan Jew, and Demian Sainz. The staff truly goes above and beyond to help us have a successful graduate life, and they were a key part of my decision to attend UCSF. In addition, I would like to express my appreciation for Elana Lewis and

Bethany Taylor, who have made administrative procedures simple and efficient in Gladstone.

I would like to give special thanks to Joe, who has provided great support and encouragement during my final lap of graduate school. Thank you for having faith in me, and always cheering me on to do my best.

Finally, I would like to acknowledge many others who have helped me along the way, who I may not have specifically named above. I genuinely appreciate everyone who has been part of my life the past six years, and thank you for making this work possible.

Contributions to thesis work

Chapter 2 is adapted from a manuscript in preparation, and the work is done under the supervision of Benoit Bruneau. Alec Uebersohn performed the ChIP-Seq experiments and initial analysis, and Daniel He worked on pilot experiments for ChIP-Seq. The Gladstone Bioinformatics Core, Genomics Core, Stem Cell Core and Histology Core also provided technical support for multiple aspects of the project. Ji-Eun Lee and Kai Ge contributed the *Kmt2d*$^{fl/fl}$ mouse line.

An essential role for H3K4 methyltransferase KMT2D in heart development

by Siang Yun Ang

Abstract

Heart development is a complex process that requires tightly regulated cardiac gene expression. One important control is through dynamic changes in chromatin structure. Methylation of histone H3 lysine 4 (H3K4) has been linked to transcriptional activation at associated gene loci. Mutations in *KMT2D* (*MLL2*/*ALR*), which encodes for an H3K4 methyltransferase, lead to Kabuki syndrome, and patients present with congenital heart defects. We hypothesize that *Kmt2d*, and thus H3K4 methylation, are required for normal cardiac gene expression and heart development.

Although *KMT2D* haploinsufficiency causes Kabuki syndrome in humans, mice lacking one allele of *Kmt2d* develop through adulthood with normal cardiac morphology and function. To define the requirement for *Kmt2d* in cardiogenesis, we deleted *Kmt2d* in mesodermal precursors and anterior heart field precursors. Mesodermal deletion of *Kmt2d* led to embryonic lethality at E10.5 with severely hypoplastic hearts, whereas deletion in the anterior heart field led to embryonic lethality at E13.5 with outflow tract abnormalities and ventricular septal defects (VSDs). To determine the cell type responsible for these cardiac defects, we

deleted *Kmt2d* in the myocardium, which led to embryonic lethality at E14.5 with VSDs and thin compact myocardium.

Specific gene expression programs were dysregulated in each deletion mutant, indicating that *Kmt2d* regulates distinct gene subsets in different cardiac cell populations. Interestingly, gene expression analysis revealed common overrepresented GO categories between the three cardiac deletion mutants, including downregulation of ion transport genes and upregulation of hypoxia response genes.

We further determined that myocardial deletion of *Kmt2d* leads to a decrease in H3K4me2 levels at promoters and at H3K27Ac-enriched enhancers. H3K4me1 levels were also decreased at enhancers, but H3K4me3 levels remained unchanged. Comparison with gene expression data revealed that multiple ion transport genes had decreased H3K4me2 and decreased expression in the absence of *Kmt2d,* suggesting a novel role for KMT2D in the regulation of ion transport genes via H3K4 di-methylation.

Overall, our work demonstrates a critical requirement for *Kmt2d* in cardiac precursors and myocardium during embryonic development. Our results also indicate that KMT2D, through its role as a H3K4 di-methyltransferase in the myocardium, is essential for regulating cardiac gene expression during heart development.

Table of Contents

List of figures

List of tables

Chapter 1

Introduction

Introduction

The heart is the first functional organ in the embryo, responsible for pumping blood through the circulatory system to deliver nutrients and oxygen to all cells in the body. Therefore, proper cardiac morphogenesis and heart function is crucial during embryonic development.

Heart development is a complex process that requires tightly regulated gene expression, and aberrant cardiac gene expression underlies the majority of congenital heart defects (CHDs). CHDs are among the most common birth defects, affecting approximately 9 in 1,000 children (Linde et al., 2011). However, the etiology of most CHDs remains unclear, highlighting the importance of understanding how genetic networks are controlled during heart development.

Overview of heart development

Shortly after gastrulation at embryonic day 6.5 (E6.5), cardiac progenitor cells start migrating to the anterior and lateral regions of the developing embryo (Moorman & Christoffels, 2003). These progenitors colonize the splanchnic mesoderm, giving rise to two lateral cardiac fields. At E7.5, a population of cardiac progenitors, also known as the primary heart field, migrates anteriorly and converges at the ventral midline, forming the cardiac crescent (Buckingham et al., 2005). Another population of cardiac progenitors, also known as the

secondary or anterior heart field (AHF), is located medial and anterior to the primary field (Harvey, 2002).

At E8.0, the medial region of the cardiac crescent migrates to bring the two lateral cardiac cell populations together to form a linear beating heart tube (Olson, 2006). The secondary/anterior heart field population then migrates to the anterior and posterior of the heart tube, eventually contributing to the right ventricle, outflow tract and ventricular septum (Mjaavedt et al., 2001; Waldo et al., 2001; Kelly et al., 2001). At 9.5, the heart starts remodeling to form the cardiac chambers, looping rightwards to realign the caudal region of the cardiac tube and to bring inflow and outflow segments to the anterior pole of the heart (Christoffels et al., 2000). By 10.5, looping morphogenesis is almost complete, and the cardiac chambers show the first signs of septation. Cardiac neural crest cells migrate to the outflow tract, eventually contributing to the outflow tract septum (Jiang et al., 2000).

Between E11.5 and E14.5, the outflow tract septates into the pulmonary artery and aorta (Restivo et al., 2006), as endocardial cushions fuse to form atrioventricular canals (Gitler et al., 2003). The septum primum and the subsequent septum secundum develop in the atria, completing atrial septation. The interventricular septum begins as a muscular ridge on the floor of the ventricles, eventually fusing with the endocardial cushions, giving rise to the membranous and muscular components of the interventricular septum (Lin et al.,

2012). The ventricular myocardium proliferates actively during this period, contributing to a major increase in thickness of the ventricular wall. Remodeling of the cardiac chambers, as well as formation of the valves and major septation events, give rise to a definitive four-chambered heart by E14.5 (Samsa et al., 2013).

Epigenetic modifiers control cardiac gene expression and heart development

The genetic networks controlling heart development has been well studied, with particular focus on signaling pathways that are responsible for cardiac morphogenetic events and transcription factors that regulate cardiac gene expression (Olson, 2006; Bruneau, 2008). Mutations in key cardiac transcription factors frequently result in heritable CHDs (Clark et al., 2006), indicating the importance of tightly controlled cardiac gene expression.

In the eukaryotic cell, control of gene expression occurs at several levels, including transcriptional regulation and chromatin structure. In recent years, it has emerged that dynamic changes in chromatin structure are critical in controlling cardiac gene expression (Chang & Bruneau, 2012). The two types of chromatin modifiers that have been implicated in heart development are chromatin remodelers, which utilize energy from ATP hydrolysis to move nucleosomes (Bruneau, 2010), and histone modifying enzymes, which catalyze

covalent histone modifications to change chromatin accessibility to DNA regulatory elements (van Weerd et al., 2011; Nührenberg et al., 2014).

ATP-dependent chromatin remodeling complexes, such as the enzyme *Brg1* and its subunits *Baf45c*, *Baf60c*, *Baf180*, have been implicated in heart development through interaction of the complex with cardiac transcription factors and signaling pathways (Hang et al., 2010; Takeuchi et al., 2011; Lickert et al., 2004; Takeuchi et al., 2009; Wang et al., 2004). Histone methylases and demethylases, such as *Smyd1* and *Whsc1*, are also known to associate with cardiac transcription factors to control cardiac gene expression (Park et al., 2010; Sims et al., 2002; Nimura et al., 2009). In absence of these histone modifiers, mouse mutants have dysregulated cardiac gene expression, resulting in various cardiovascular defects and disrupted cardiac function. These results demonstrate critical roles for chromatin regulators in the control of cardiac gene expression and cardiac morphogenesis. Thus, understanding epigenetic regulation of heart development could provide insights into the etiology of CHDs.

Histone H3 lysine 4 (H3K4) methylation and its emerging role in heart development

Histone H3 lysine 4 (H3K4) methylation has been linked to transcriptional activation in multiple eukaryotic species. Lysine residues can be mono-, di-, or tri-

methylated, with each histone mark associated with specific regulatory elements and biological functions (Ruthenburg et al., 2007).

H3K4 mono-methylation (H3K4me1) is associated with enhancer regions, which are cis-regulatory elements that affect gene transcription and may be located up to hundreds of kilobases (kb) away from its target of regulation. H3K4me1 enrichment, along with p300 and H3K27Ac enrichment, are marks of active enhancers that contribute to tissue-specific transcriptional activity of its regulatory targets (Creyghton et al., 2010).

In contrast, H3K4 di-methylation (H3K4me2) is enriched in the region ± 1 kb surrounding the transcriptional start site (TSS), or spread across a large area within the gene body. In yeast, it has been proposed that H3K4me2 recruits the Set3 complex to facilitate histone deacetylation downstream of the TSS, which may promote efficient elongation by RNA polymerase II. Multiple studies in human and mouse $CD4^+$ T cells, retina, erythroblasts and brains have revealed that H3K4me2 enrichment within the gene body is a unique chromatin property of tissue-specific genes, associated with intragenic enrichment of other cis-regulatory elements. (Kim & Boratowski, 2009; Pekwoska et al., 2010; Wong et al., 2011; Popova et al., 2012)

H3K4 tri-methylation (H3K4me3) is highly enriched and localized in the region ± 1 kb surrounding the TSS. This histone mark is enriched at the 5' end of almost

all actively expressed genes, and is strongly correlated with transcription rates, active polymerase II occupancy and histone acetylation. H3K4me3 has been shown to interact with transcription factor II D (TFIID) complex, enhancing transcription by stimulating preinitiation complex formation (Lauberth et al., 2013). The diversity and variation of H3K4 methylation patterns, as well as its crosstalk with other histone modifications and transcriptional machinery, indicates a complex control of active gene transcription and tissue-specific gene expression.

In mammals, H3K4 methylation is established by at least seven methyltransferases, each of which contain a SET domain that catalyzes the addition of methyl groups to the H3K4 residue. These methyltransferases include SET1A, SET1B and five members of the KMT2 lysine methyltransferase family (KMT2A-E), originally named the mixed lineage leukemia (MLL1-5) proteins (Eissenberg et al., 2010; Shilatifard, 2012). These enzymatic isoforms exist in multi-subunit complexes, with non-enzymatic subunits conferring enhanced catalytic activity and tissue specificity. Deletion mutants of the methyltransferases have distinct lethal phenotypes, indicating that they are non-redundant and are specialized for regulating specific gene expression programs during development.

A study of *de novo* mutations in severe CHD cases showed a significant over-representation of genes related to H3K4 methylation (Zaidi et al., 2013). This

includes genes required for the production, removal or reading of H3K4 methylation, which demonstrates the importance of H3K4 methylation in heart development. In particular, this includes a nonsense mutation predicted to result in haploinsufficiency of the H3K4 methyltransferase, *KMT2D*, suggesting a possible specific role for *KMT2D* in heart development.

KMT2D **and congenital heart defects in Kabuki Syndrome**

KMT2D is also known as *MLL2*, *MLL4*, or *ALL-1* related gene (*ALR*). The nomenclature confusion arose due to the simultaneous naming of *MLL2* for the human gene on chromosome 12q13.12 by the HUGO Gene nomenclature committee, which was also adopted by FitzGerald and Diaz (1999) for the human gene on chromosome 19q13.12. Both genes were also subsequently referred to as *MLL4*, adding to the confusion. As a result, the mouse ortholog of the human chromosome 12 gene (MGI:2682319, chromosome 15), which is named *Mll2* by the Mouse Genomic Nomenclature Committee, has also been referred to as *Mll4* in literature. For clarity, the use of *KMT2D*/*Kmt2d* has been suggested (Bögershausen n et al., 2013) to refer to the human gene on chromosome 12 and the mouse gene on chromosome 15. This naming follows the comprehensive nomenclature system proposed by Allis et al. (2007), which renames all methyltransferases based on phylogenetic relationships.

Ng et al. (2010) first identified *KMT2D* mutations as a cause of Kabuki Syndrome, a rare syndrome characterized by a distinctive facial appearance and multiple developmental anomalies that include cardiac defects (Matsumoto & Niikawa, 2003; Adam & Hudgins, 2005). Since then, more than 520 cases of Kabuki Syndrome have been examined, revealing that about 70% of Kabuki Syndrome individuals have mutations in *KMT2D* (Paulussen et al., 2010; Hannibal et al., 2011; Li et al., 2011; Micale et al., 2011; Banka et al., 2013, Makrythanasis et al., 2013, Miyake et al., 2013, Yoon et al., 2015). A majority of the mutations are nonsense mutations predicted to truncate KMT2D prematurely before the SET domain and result in haploinsufficiency.

About 60% of Kabuki Syndrome patients are diagnosed with CHDs, with a varying spectrum of cardiac malformations (Digilio et al., 2001, Yuan et al., 2013, Yoon et al., 2015). The most frequent CHDs are aortic coarctation (23%), atrial septal defects (ASDs, 20%), and ventricular septal defects (VSDs, 17%). These congenital cardiac defects, as well as left-side heart anomalies, are observed in Kabuki Syndrome patients with *KMT2D* mutations (Ng et al., 2010; Yoon et al., 2015) indicating the importance of *KMT2D* in heart development.

In addition, Pax transactivation-domain interacting protein (PTIP), a KMT2D complex specific subunit that mediates recruitment of KMT2D to specific genes (Cho et al., 2007), is required for the stability of a transcriptional program in adult murine cardiomyocytes. Deletion of the gene encoding PTIP in adult

cardiomyocytes leads to arrhythmias, due to reduction in H3K4me3 altering the gene expression of the ion-channel subunit-encoding genes *Kcnip2* (Stein et al., 2011). These data suggest that the KMT2D complex is involved in cardiogenesis and required for normal heart function, and insights into the role of KMT2D in heart development would be useful for understanding epigenetic regulation of cardiac gene expression.

KMT2D acts as a H3K4 mono-, di- or tri-methyltransferase depending on cellular context

Studies in various tissues from humans, mice and fruit flies have demonstrated that KMT2D is a H3K4 methyltransferase and is a key regulator of gene expression during development and disease. However, there is no consensus on whether KMT2D acts as a H3K4 mono-, di-, or tri-methyltransferase. Instead, these studies indicate that KMT2D may catalyze any of these modifications depending on the cell type, and the role of KMT2D may be dependent on its cellular and temporal context.

In *Drosophila*, there are two *KMT2D* homologs, trithorax-related (Trr) and cara mitad (cmi). Both genes are essential for Drosophila development and act as H3K4 mono-methyltransferases at enhancers. Loss of Trr leads to global H3K4me1 loss in various tissues (Herz et al., 2012), whereas cmi is required for the proper regulation of hormone dependent genes during development

(Chauhan et al., 2013). Similarly in human cancer cell line HCT116 and mouse embryonic stem (ES) cells, KMT2D was preferentially found at enhancer regions, and loss of *KMT2D* in HCT116 cells led to a bulk reduction in H3K4me1 (Guo et al., 2013). These findings suggest that *KMT2D* regulates enhancer activity through its role as a H3K4 mono-methyltransferase.

In addition, *Kmt2d* was identified to be essential for mouse adipogenesis, which uncovered an additional role for *Kmt2d* as a mono- and di-methyltransferase (Lee at al., 2014). There is an increase in KMT2D occupancy at adipogenic enhancers during adipocyte differentiation, and loss of *Kmt2d* results in a global decrease in H3K4me1 and H3K4me2 at these enhancers. This result suggests that KMT2D is required for maintaining H3K4me1 and H3K4me2 levels at enhancers, and its loss could result in defects in enhancer activation and cell-type-specific gene expression.

In contrast, mice with a genetrap allele of *Kmt2d* have a decrease in H3K4me3 levels in the dentate gyrus (Bjornsson et al., 2014), suggesting that *Kmt2d* is required for its H3K4 tri-methyltransferase activity during neurogenesis. In Wan et al. (2014), *Kmt2d* knockdown in mouse ES cells that were subsequently differentiated to embryoid bodies (EBs) show that *Kmt2d* deficiency impairs differentiation towards the mesendoderm lineages, but it is dispensable for ectoderm differentiation. KMT2D enrichment is found by ChIP-qPCR at cardiac-specific promoters, such as *Nkx2-5, Baf60c* and *Tbx5*. *Kmt2d* deficiency in

differentiating EBs decreased H3K4me3 at these promoter regions, indicating *Kmt2d* is required to maintain H3K4me3 levels at promoters of specific cardiac genes. However, there are significant differences between *in vivo* heart development and *in vitro* cardiac differentiation, such as 3D morphogenetic events, hemodynamic effects, and tissue signaling gradients. Therefore, although this study suggests *Kmt2d* is required for H3K4 tri-methylation of specific cardiac gene promoters in differentiating EBs, the results observed in *in vitro* EB differentiation may not be able to effectively predict the role of KMT2D in heart development.

Depending on the cellular context, we observed that KMT2D may act either as a H3K4 mono-methyltransferase or di-methyltransferase at enhancers, or as a H3K4 tri-methyltransferase at the promoter regions, to regulate tissue specific gene expression during key developmental events. Together, based on the studies described above, we hypothesize that *Kmt2d* has a critical role in maintaining H3K4 methylation levels in the developing heart and thus controlling cardiac gene expression.

Chapter 2

Kmt2d regulates cardiac gene expression during heart development via H3K4 di-methylation

Results

Single copy of *Kmt2d* is sufficient for normal heart development and function

We examined the expression of KMT2D in the developing embryonic heart. *Kmt2d* transcript was expressed at similar levels during embryonic development and increased almost two-fold at birth (Figure 1A). Immunofluorescence for KMT2D on sections from E12.5 hearts confirmed expression in cardiomyocytes and endocardial cells (Figure 1B).

Kabuki syndrome patients carry truncating mutations in *KMT2D*, which are predicted to result in non-functional KMT2D protein, or haploinsufficiency. To determine if *Kmt2d* is haploinsufficient in mice, mice carrying a floxed allele of *Kmt2d* (*Kmt2d*^{fl}, referred to as *Mll4*^{fl} in Lee at al., 2014) were crossed to a transgenic mouse line that expresses Cre recombinase under the control of a human beta actin Cre promoter (*ACTB-Cre*, Lewandoski et al., 1997) to generate mice heterozygous for a *Kmt2d*$^{\Delta}$ null allele. As controls, we used *Kmt2d*$^{+/+}$ littermates. Quantitative PCR confirmed depletion of the *Kmt2d* transcript by 50% in E8.0 *Kmt2d*$^{\Delta/+}$ mutant embryos (Figure 1C). *Kmt2d*$^{\Delta/+}$ mice survived to adulthood.

To assess whether *Kmt2d*$^{\Delta/+}$ mice would present with cardiac defects observed in Kabuki syndrome patients, we examined *Kmt2d*$^{\Delta/+}$ mice and wild-type controls at postnatal day (P) 35. *Kmt2d*$^{\Delta/+}$ mice did not have alterations in heart weight/body weight compared with controls (Figure 1D), and detailed histological examination of *Kmt2d*$^{\Delta/+}$ and control hearts showed no differences in cardiac morphology (Figure 1E, Figure S1A). To determine if *Kmt2d*$^{\Delta/+}$ mice had altered cardiac function, we performed echocardiography on P35 *Kmt2d*$^{\Delta/+}$ and wild-type controls. We determined that there were no significant changes in ejection fraction, fractional shortening, stroke volume or cardiac output (Figure 1F-1H, Figure S1B-1C). However, we observed that diameter of the ascending aorta was narrower and the aortic valve peak velocity was increased in *Kmt2d*$^{\Delta/+}$ mutants (Figure 1I to 1J).

Therefore, we conclude that a single copy of *Kmt2d* is sufficient for normal heart development and function, with mild defects in the ascending aorta.

Conditional deletion of *Kmt2d* in cardiac precursors and myocardium disrupt cardiac development

To determine if *Kmt2d* was required for heart development, we interbred *Kmt2d*$^{\Delta/+}$ animals to obtain homozygous *Kmt2d*$^{\Delta/\Delta}$ embryos. No live *Kmt2d*$^{\Delta/\Delta}$ offspring were observed (Table 1), and *Kmt2d*$^{\Delta/\Delta}$ embryos recovered at E8.0 lacked somite pairs and a headfold (Figure 2A). Quantitative PCR confirmed

depletion of *Kmt2d* in *Kmt2d*$^{\Delta/\Delta}$ mutants (Figure S2A). Severe morphological defects in the *Kmt2d*$^{\Delta/\Delta}$ embryos indicated an early requirement of *Kmt2d*, precluding assessment of its role during heart development. We therefore used conditional deletion of *Kmt2d* to investigate its role in specific cardiac populations (Figure 2B).

To determine if *Kmt2d* was required in cardiac precursors, we generated *Kmt2d*-deficient mice using the *Mesp1*^{Cre} driver, which is expressed in mesodermal precursors (Saga et al., 1999) and the *Mef2cAHF::Cre* driver, which is expressed in anterior heart field (AHF) precursors (Verzi et al., 2005) (Figure 2B). Quantitative PCR confirmed a significant decrease of the *Kmt2d* transcript in the embryonic hearts of E9.0 mesodermal deletion mutants and E11.5 AHF deletion mutants (Figure S2B, S2C).

To verify that the Cre deletion leads to a loss of KMT2D protein, we included in our breeding scheme a Cre reporter allele, *Rosa*^{mTmG} (Muzumdar et al., 2007). This reporter includes a membrane targeted tdTomato (mT) cassette under the ubiquitous Rosa promoter, which is excised in the presence of Cre recombinase to allow expression of a membrane targeted green fluorescent protein (mG). Immunostaining of E10.5 *Mef2cAHF::Cre;Kmt2d*$^{fl/fl}$*;Rosa*$^{mTmG/+}$ mutant hearts exhibited reduced KMT2D levels in GFP positive cells, where Cre recombinase is expressed (Figure 2E).

No live *Mesp1*^{Cre}*;Kmt2d*$^{fl/fl}$ mutants were recovered after E10.5 (Table 1). E10.5 mutants appeared developmentally delayed, exhibiting pericardial edema and a linear heart tube (Figure 2F-G). Similarly, no live *Mef2cAHF::Cre;Kmt2d*$^{fl/fl}$ offspring were observed. *Mef2cAHF::Cre;Kmt2d*$^{fl/fl}$ mice were found at Mendelian ratios until E11.5, and this decreased subsequently, with embryonic lethality by E13.5 (Table 1, Figure S2D). Examination of serial histological sections of E12.5 mutant hearts revealed thin compact myocardium and reduced trabeculation (Figure 2F). Examinations of the gross E12.5 mutant hearts show failure of outflow tract septation into the aorta and pulmonary artery (Figure 2G). The cardiac defects of both genotypes indicated that *Kmt2d* is required in cardiac precursors for heart development.

Since mesodermal and AHF precursors contribute to both endocardium and myocardium, we wanted to determine if *Kmt2d* was required in the myocardium. We deleted *Kmt2d* in the myocardium using *Tnnt2::Cre* driver, which is expressed in the embryonic myocardium from E7.5 onwards (Jiao et al., 2003), and quantitative PCR confirmed a significant decrease of *Kmt2d* transcript in E11.5 hearts (Figure S2E). *Tnnt2::Cre;Kmt2d*$^{fl/fl}$ embryos were found at Mendelian ratios until E13.5, but no live mutants were observed after E14.5 (Table 1, Figure S2F). Examination of serial histological sections of the E12.5 mutant hearts revealed thin compact myocardium and reduced trabeculation (Figure 2H), similar to the AHF precursor deletion phenotype. However,

myocardial deletion mutants show normal septation of the outflow tract into the aorta and pulmonary artery (Figure 2H).

Hypoplasia of the compact myocardium in *Tnnt2::Cre;Kmt2d*$^{fl/fl}$ mutants suggested decreased cardiomyocyte proliferation. To test this hypothesis, we performed cell cycle analysis on E12.5 control and mutant hearts (n=3 each), sorting for Cre-positive cells with GFP fluorescence. In the controls, 66% of the Cre-positive cell population was in the G2/M phase, but in the mutants only 58% of the cell population was in the G2/M phase (Fig 2I). This indicated that a portion of cells is arrested in G1 and S phases, which could contribute to hypoplasia of the compact myocardium.

Taken together, we conclude that *Kmt2d* is required in cardiac precursors and myocardium during heart development, with the distinct phenotypes suggesting *Kmt2d* plays separate and essential roles in each cardiac population.

Loss of *Kmt2d* leads to downregulation of ion transport genes and upregulation of hypoxia response genes

To assess the transcriptional consequences of *Kmt2d* loss during heart development, we performed global gene expression analyses of embryonic hearts with *Kmt2d* deletion in cardiac mesoderm, AHF precursors and myocardium. For *Mesp1*^{Cre} crosses, we used four biological replicates each of

control and mutant E9.0 hearts. For *Mef2cAHF::Cre* and *Tnnt2::Cre* crosses, we used three biological replicates each of control and mutant E11.5 hearts.

We found that there were 306 genes dysregulated in *Mesp1*^{Cre} mutants (in dark blue) at FDR<0.1, 340 genes dysregulated in *Mef2cAHF::Cre* mutants (in blue), 758 genes dysregulated in *cTnT-Cre* mutants (in teal) at FDR<0.05. Average-linkage cluster analysis showed that differentially expressed genes in *Mesp1*^{Cre}*, Mef2cAHF::Cre* and *Tnnt2::Cre* mutants clustered separately (Figure 6A), indicating that *Kmt2d* regulates distinct subsets of genes in each cardiac population. Interestingly, gene ontology analysis revealed that the different subsets of genes upregulated in the three deletion mutants were enriched for functions in hypoxia response, whereas downregulated genes were enriched for functions in ion transport and homeostasis (Figure 3A).

To determine biological functions that were commonly dysregulated in all three cardiac deletion mutants, we analyzed this dataset using Ingenuity Pathway Analysis. We observed that common dysregulated biological functions included muscle contractility, molecule transport and ion homeostasis (Figure 3B). In addition, myeloid cell movement and inflammatory response functions were dysregulated (Figure S3A), likely due to the decrease of red blood cells and hypoxia in the mutant hearts secondary to circulatory failure.

Predicted disease associations included heart failure and myocardial infarction (Figure 3C), suggesting strong disruption of cardiac function and circulatory failure. We also observed that predicted dysregulation of upstream regulators included multiple hypoxia response genes, such as HIF1A and COMMD1 (Figure S3B).

We analyzed the *Tnnt2::Cre* deletion gene expression dataset further using an unbiased gene set enrichment analysis (GSEA) (Subramanian et al., 2005). We observed a significant decrease in inorganic anion transport genes (Figure 3D) and erythropoietic markers, as well as an enrichment of hypoxia response genes (Figure S3C).

To determine if the decrease in ion transport gene expression was due to a cell autonomous effect, we examined the expression of ATP1A2, the alpha-2 isoform of the Na^+,K^+-ATPase. We found that ATP1A2 was decreased in Cre-positive mutant cardiomyocytes (Figure 3E). In contrast, HIF1A, a key hypoxia response factor was mostly increased in Cre-negative cells (Figure S3D), indicating that the increase in hypoxic response gene expression is due to a non-cell autonomous effect.

Changes in ion transport and homeostasis likely led to decreased cardiac function, which decreased transport of red blood cells and oxygen in the embryo. We observed a non-cell autonomous hypoxia response, which suggests that

hypoxia is a secondary effect of circulatory failure. Fetal heart development has been shown to be susceptible to hypoxic stress, causing hypoxic mutants to develop cardiac defects, such as thin compact myocardium and septal defects (Ream et al., 2008, Yin et al., 2002). This is similar to what we observe in the *Kmt2d* deletion mutants, and may reflect a downstream effect of chronic heart failure.

Therefore, we conclude that although *Kmt2d* regulates distinct subsets of genes in mesodermal precursors, AHF precursors and cardiomyocytes, its loss leads to a decrease in ion transport gene expression and an increase in hypoxia response. Further examination of myocardial deletion mutants also revealed that the increase in hypoxia response may be secondary to cardiac and circulatory failure.

Myocardial deletion of *Kmt2d* results in decrease in H3K4me2 at ion transport genes

Since *Kmt2d* is a H3K4 methyltransferase, we next sought to determine if myocardial deletion of *Kmt2d* led to changes in H3K4 methylation levels. Thus, we performed chromatin immunoprecipitation (ChIP) using antibodies to H3K4me1, H3K4me2 and H3K4me3 on E11.5 control (n=90) and mutant hearts (n=90). We then examined the enrichment of the histone marks at the

transcriptional start site (TSS) and non-TSS H3K27Ac bound sites, which marks active enhancers (Nord et al., 2013).

Average profile plots revealed a significant decrease in H3K4me2 levels at the TSS and at non-TSS H3K27Ac sites (Figure 4A, blue and red lines). However, there were no significant changes in the levels of H3K4me1 and H3K4me3 at the TSS. Similarly at non-TSS H3K27Ac sites, there were no significant changes in H3K4me3 levels, although there was a modest decrease in H3K4me1 levels.

Clustering analysis of ChIP-Seq peaks indicated that H3K4me2 peaks clustered tightly into control and mutant groups, whereas H3K4me1 and H3K4me3 peaks did not (Figure S4A). This demonstrates a consistent difference in H3K4me2 profiles between control and mutants, with more variability amongst the H3K4me1 and H3K4me3 profiles.

We further examined average profile plots for the 482 genes that were downregulated in the myocardial deletion mutants. We observed a marked decrease in H3K4me2 at the TSS and non-TSS H3K27Ac sites, with less noticeable differences in H3K4me1 and H3K4me3 (Figure 4A, green and orange lines). This is similar to the global pattern, although these genes have higher average levels of H3K4me1 and H3K4me2 at both the TSS and non-TSS H3K27Ac sites compared to the global average.

Overall, we identified 6699 regions with decreased H3K4me2 (Figure 4B, in red). 11.73% of these regions did not map to any gene, whereas 54.84% mapped to 1 gene and 33.24% mapped to 2 genes (Figure S4B). A negligible percentage mapped to 3 genes or more. 52.72% of region-gene associations were located within 5 kb of the TSS, whereas 31.28% were located within 5 to 50 kb and 15.90% were located within 50 to 500 kb (Figure S4C). This indicates an approximately equal distribution of regions with decreased H3K4me2 at proximal and distal regulatory elements.

Of the regions with decreased H3K4me2, 211 corresponded to 166 genes that were downregulated in myocardial deletion mutants (Figure 4B, in orange). Gene ontology analysis showed that ion transport related genes were significantly enriched in this subset of 166 genes (Figure 4C). In the absence of *Kmt2d*, ion transport related genes, such as *Atp1a2* and *Fxyd1*, exhibited decreased gene expression and decreased H3K4me2 levels at the TSS and throughout the gene body (Figure 4D). Most genes with decreased me2 did not show significant changes in gene expression, suggesting gene expression regulation by *Kmt2d*-dependent H3K4 di-methylation is highly specific. On the other hand, we find that genes with decreased gene expression are significantly more likely to be associated with decreased H3K4me2 regions (hypergeometric test $p = 1.10 \times 10^{-18}$).

We also identified a smaller number of 2730 regions with decreased H3K4me1. 21.76% of these regions did not map to any gene, whereas 40.92% mapped to 1 gene and 37.29% mapped to 2 genes (Figure S5A). 6.11% of region-gene associations were located within 5 kb of the TSS, whereas 60.29% were located within 5 to 50 kb and 35.59% were located within 50 to 500 kb (Figure S5B). This indicates that most of the regions with decreased H3K4me1 were located at distal regulatory elements. The smaller number of regions with decreased H3K4me1 levels also suggests that KMT2D plays a greater role in maintaining H3K4me2 levels and to a lesser extent, H3K4me1 levels.

We also observed a similar trend with decreased H3K4me1 regions, with 120 regions corresponding to 77 genes that were downregulated in myocardial deletion mutants (Figure S5C, in blue and orange). Gene ontology analysis also showed a significant enrichment of ion transport related genes in this subset of 77 genes (Figure S5D). Most genes with decreased H3K4me1 levels did not show significant changes in gene expression, suggesting gene expression regulation by *Kmt2d*-dependent H3K4 mono-methylation is also highly specific. On the other hand, genes with decreased gene expression are significantly more likely to be associated with decreased H3K4me1 regions (hypergeometric test $p = 1.25 \times 10^{-13}$).

Interestingly, only 172 regions have reductions in both H3K4me1 and H3K4me2 levels, corresponding to 6.30% of regions with decreased H3K4me1 or 2.57% of regions with decreased H3K4me2 (Figure S5C). Of these 172 regions, only 7 mapped to downregulated genes. This suggests that KMT2D has distinct roles in maintaining H3K4me1 and H3K4me2 levels at different genomic regions. No significant decrease in H3K4me1 and H3K4me3 levels are observed at the TSS of *Atp1a2* despite a significant decrease in H3K4me2 levels (Figure S5E), further illustrating KMT2D is highly specific in regulating H3K4me2 levels at these genomic loci.

Taken together, these results demonstrate that KMT2D is an essential H3K4 di-methyltransferase in the developing heart, with a minor role as a H3K4 mono-methyltransferase. The results also indicate that KMT2D is required to maintain H3K4me2 marks for the stability of a transcriptional program associated with ion homeostasis in the myocardium.

Discussion

H3K4 methylation, a histone mark associated with transcriptionally active chromatin regions, has been shown to be essential for regulation of developmental gene expression. Studies of patients with severe *de novo* congenital heart disease establish that mutation in genes involved in the H3K4 methylation pathway disrupt heart development (Zaidi et al., 2013), implicating this active chromatin mark in the regulation of cardiac gene expression during development. However, very little is understood about how H3K4 methylation may regulate key transcription programs during cardiogenesis. Additionally, Kabuki Syndrome cases with mutations in the H3K4 methyltransferase *KMT2D* and a high prevalence of CHD indicate that *KMT2D* is required for normal cardiac morphogenesis (Ng et al, 2010; Yoon et al., 2015), but its function in heart development is not known.

Our study demonstrates that *Kmt2d* is essential for H3K4 methylation during heart development to regulate an active transcription program associated with ion transport. We defined the specific and temporal requirement of *Kmt2d* in the cardiac mesoderm, AHF precursors and cardiomyocytes. We further identified a dysregulated transcriptional program depleted for ion transport regulators and enriched for hypoxia response genes in the *Kmt2d* deletion mutants. Finally, we determined that *Kmt2d* is required primarily to maintain H3K4me2 levels at the TSS and enhancers at multiple genomic loci, including several genes

downregulated in absence of *Kmt2d*. We also observed a decrease in H3K4me1 in a smaller number of enhancer regions. These results are consistent with KMT2D playing an important role in the developing heart as a H3K4 di-methyltransferase, as well as a more minor role as a H3K4 mono-methyltransferase, to regulate cardiac gene expression.

Previous studies have mostly focused on *Kmt2d* as a H3K4 mono-methyltransferase at enhancer regions or as a H3K4 tri-methyltransferase at promoter regions (Guo et al., 2013; Lee at al., 2014; Bjornsson et al., 2014; Wan et al., 2014). Although Lee at al. (2014) explored the role of *Kmt2d* as H3K4 di-methyltransferase, they found that *Kmt2d* is required for enhancer activation during differentiation. Our results indicate that *Kmt2d* is a H3K4me2 methyltransferase required both at enhancers and promoters for active gene expression, identifying a novel role for *Kmt2d*.

Most of our current understanding of H3K4 methylation has also been focused on H3K4me1 and H3K4me3, with little understood about the dynamics of H3K4me2 and H3K4 di-methyltransferases (Ruthenburg et al., 2007; Shilatifard, 2012). Recent studies revealed that H3K4me2 levels are enriched in the gene body of tissue specific genes, suggesting H3K4me2 plays a key role in regulating tissue specific gene expression. We observe an over-representation of ion transport genes that require *Kmt2d* for H3K4me2 methylation and gene expression,

establishing the importance of H3K4me2 regulation of a cardiac-specific transcriptional program associated with ion transport.

Interestingly, although we observed a large number of genomic regions with decreased H3K4me2 and a smaller number of regions with decreased H3K4me1, only a small subset of genes was downregulated. This suggests that not all genes are sensitive to a loss in H3K4me1 or H3K4me2 levels. One possible explanation is that there is a temporal delay in H3K4me2-dependent gene expression, and some of these genes may only be downregulated at a later stage in embryonic development. In addition, gene expression is coordinately regulated by multiple histone modifications and transcriptional machinery, and thus changes in H3K4me2 levels alone may not effect a direct change in expression. Further studies of genetic interactions between *Kmt2d* and other histone modifiers may provide more insights into histone crosstalk and epigenetic regulation of gene expression.

Our findings have also uncovered multiple possible etiologies for congenital defects observed in Kabuki Syndrome patients. One of the main causes of Kabuki Syndrome is *KMT2D* haploinsufficiency, and many of these patients have CHDs. Our examination of juvenile *Kmt2d* heterozygotes exhibited narrowing of the ascending aorta, which resembles the aortic coarctation phenotype in humans. However, the atrial and ventricular septal defects observed in Kabuki Syndrome individuals were not found in these juvenile *Kmt2d* heterozygotes,

indicating that the mice model does not completely phenocopy the human syndrome. This is not surprising, as studies on the cardiac transcription factor *Nkx2-5* has revealed that haploinsufficiency in mice may not completely model human mutations (Bruneau, 2002). Multiple factors should be considered, such as variable penetrance due to the genetic background and differences in protein dosage sensitivity. Additionally, more than 200 different mutations are found across the *KMT2D* gene, adding to the complexity of the Kabuki Syndrome cardiac phenotypes and making it difficult to directly compare the mouse model against multiple human mutations. However, outflow tract septation defects in AHF deletion mutants indicate that *Kmt2d* is required for proper morphogenesis of the aorta, and directed studies could shed light on the Kabuki Syndrome aortic coarctation phenotype.

Functional ion channel activity is critical in the embryonic heart, particularly during mid-gestation. In rats treated during gestation days 9 to 14, teratogenic doses of the potassium channel blockers (e.g. almokalant, dofelitide, cisapride, and d-solatol) caused increased incidence of embryonic death (Webster et al., 1996; Abela et al., 2010; Skold et al., 2002). Examination of the embryos reveal statistically significant increased incidence of cardiac defects, particularly ventricular septal defects and great vessel abnormalities, similar to what we observed in *Kmt2d* AHF and myocardial deletion mutants. The channel blocking drugs induce embryonic cardiac arrhythmia and heart failure in the embryos, leading to chronic hypoxia-reoxygenation damage, thus adversely affecting

cardiogenesis and resulting in cardiac malformations (Wellfelt et al., 1999; Danielsson et al., 2001; Skold et al., 2001; Danielsson et al., 2007). Our results are consistent with this, as *Kmt2d* conditional deletion mutants exhibit downregulation of ion transport genes and concomitant non-cell autonomous upregulation of hypoxia response genes. Moreover, in humans, maternal use of antidepressant drugs that block the potassium channel (e.g. citalopram, clomipramine, fluoxetine, paroxetine) have been associated with an increased risk of ventricular septal defects (Pedersen et al., 2009; Kallen et al., 2006; Malm et al., 2011; Wurst et al., 2010). Therefore, it is possible that ventricular septal defects observed in Kabuki Syndrome patients could be the consequence of ion channel defects and hypoxia due to *KMT2D* haploinsufficiency during embryonic development.

In addition, cardiac conduction abnormalities and arrhythmia have been reported in a child with severe Kabuki Syndrome (Shah et al., 2005). Assessing the electrophysiological phenotype of the *Kmt2d*-deficient cardiomyocytes and changes in embryonic cardiac function of *Kmt2d* conditional deletion mutants would be useful in further understanding the role of *Kmt2d* in regulation of ion transport. This may also warrant monitoring Kabuki Syndrome patients for abnormal cardiac electrophysiology. Additionally, 10 to 40% of Kabuki Syndrome patients have epileptic seizures (Matsumoto et al., 2003; Lodi et al., 2010; Verrotti et al., 2011), which is a symptom frequently associated with

channelopathies. It would be of interest to examine if *Kmt2d* may also regulate ion homeostasis in the developing brain.

Finally, insights from our results and other studies suggest possible remedies for Kabuki Syndrome patients. Treating mice with a genetrap allele of *Kmt2d* with a histone deacetylase inhibitor, AR-42, has shown improvement in H3K4me3 levels in the dentate gyrus by restoring the balance of open chromatin states at target genes (Bjornssson et al., 2014). In another study, pretreating pregnant rats with alpha-phenyl-N-t-butylnitrone (PBN), an agent that captures reactive oxygen species, prevented formation of fetal cardiac defects caused by potassium channel blockers and subsequent hypoxia-reoxygenation damage (Wellfelt et al., 1999). Therefore, it would be interesting to determine if AR-42 or PBN could rescue the cardiac phenotypes of *Kmt2d* conditional deletion mutants. The findings will be beneficial for identifying potential therapies to treat or prevent cardiac disorders and malformations in Kabuki Syndrome cases.

Figure 1. *Kmt2d*$^{\Delta/+}$ mice have normal cardiac development but exhibit mild narrowing of the ascending aorta.

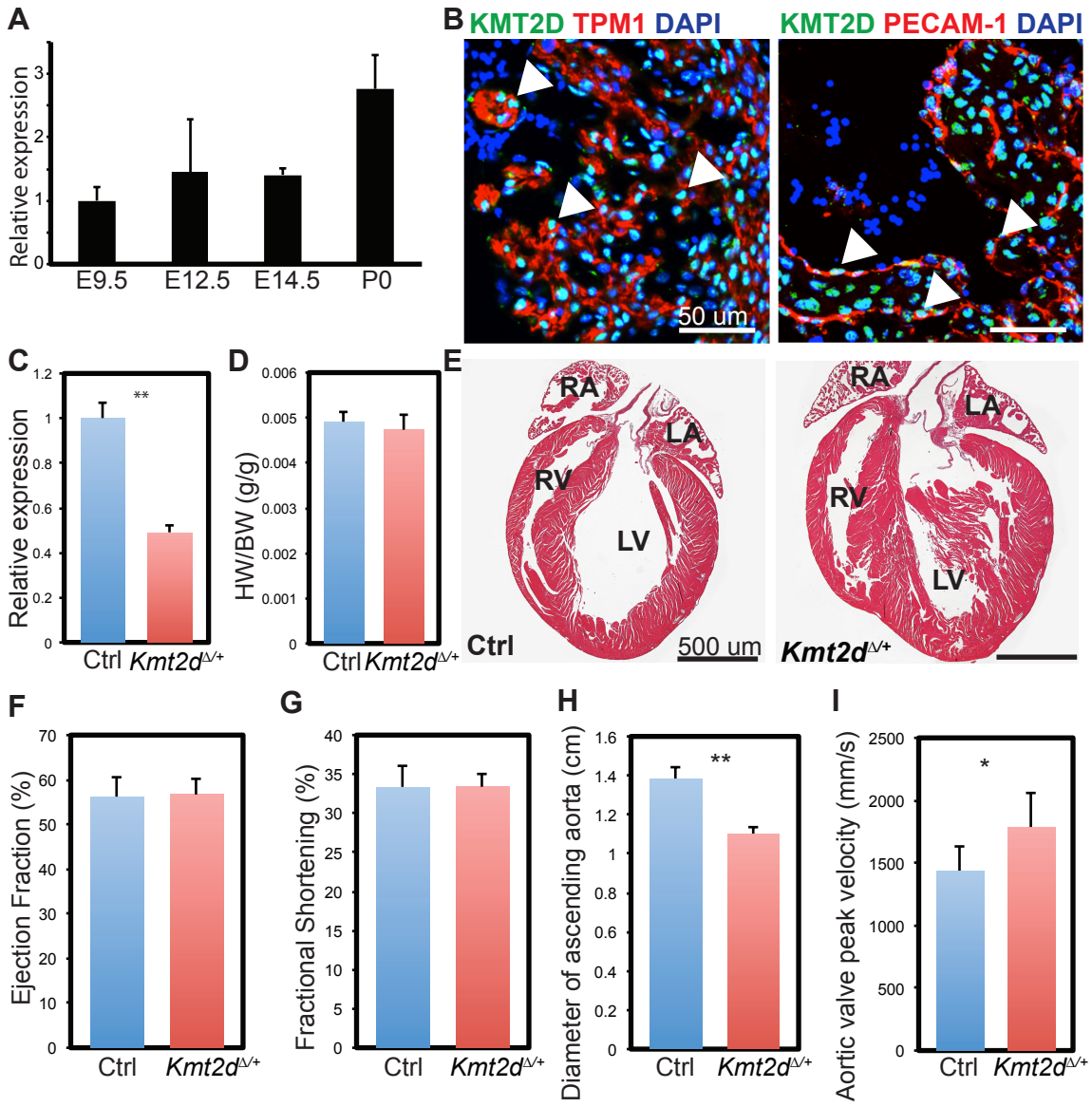

Figure 1. *Kmt2d*$^{\Delta/+}$ mice have normal cardiac development but exhibit mild narrowing of the ascending aorta.

(A) qRT-PCR of *Kmt2d* transcript levels shows that *Kmt2d* was expressed at similar levels from E9.5 to E14.5 and doubled at P0.

(B) Immunostaining shows that KMT2D is expressed in the nuclei of TPM1-expressing myocardial cells and in PECAM-1 expressing endocardial cells.

(C) qRT-PCR of *Kmt2d* transcript levels shows a 50% decrease in E8.0 *Kmt2d*$^{\Delta/+}$ mutants compared to control littermates.

(D) Heart weight to body weight ratio of P35 *Kmt2d*$^{\Delta/+}$ mutants do not show significant changes compared to control littermates.

(E) Hematoxylin and Eosin (H&E) stained cardiac sections of P35 *Kmt2d*$^{\Delta/+}$ mutants do not show observable cardiac defects compared to control littermates.

(F) Ejection fraction of P35 *Kmt2d*$^{\Delta/+}$ mutants do not show significant changes compared to control littermates.

(G) Fractional shortening of P35 *Kmt2d*$^{\Delta/+}$ mutants do not show significant changes compared to control littermates.

(H) P35 *Kmt2d*$^{\Delta/+}$ mutants exhibit a reduced diameter of ascending aorta.

(I) P35 *Kmt2d*$^{\Delta/+}$ mutants exhibit an increase in aortic valve peak velocity. (RA: Right atria; LA: Left atria; RV: Right ventricle; LV: Left ventricle; *p≤ 0.05; **p ≤ 0.01; Error bars indicate s.e.m.)

Figure 2. Deletion of *Kmt2d* in cardiac precursors and myocardium leads to embryonic lethality and cardiac defects.

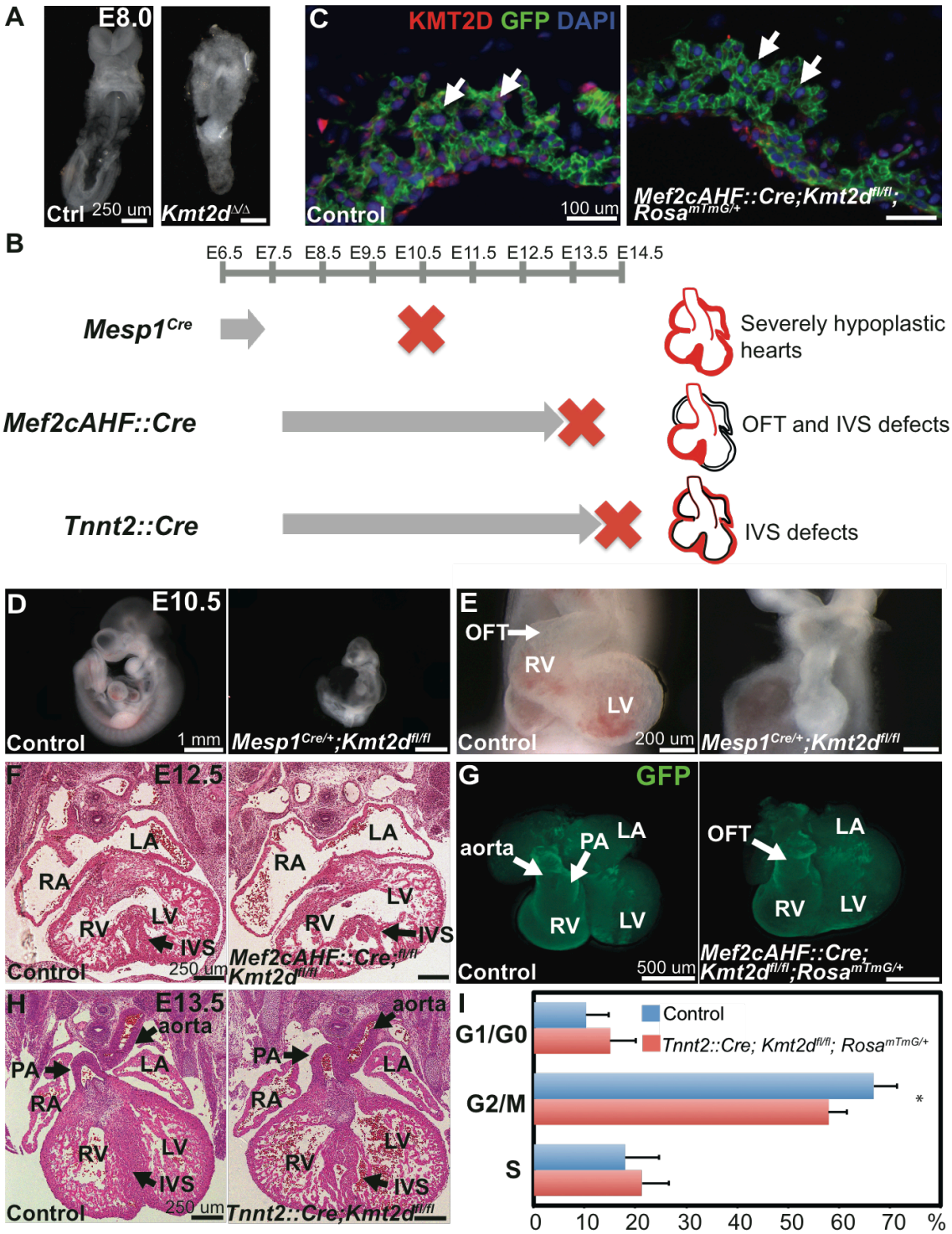

Figure 2. Deletion of *Kmt2d* in cardiac precursors and myocardium leads to embryonic lethality and cardiac defects.

(A) Representative image showing control and $Kmt2d^{\Delta/\Delta}$ mutant at E8.0. Mutant embryos lack headfolds and somites that are present in the control littermates.

(B) Overview of *Kmt2d* deletion in three cardiac populations.

$Mesp1^{Cre}$ is expressed from E6.5 to E7.5 in cardiac mesoderm precursors; deletion of *Kmt2d* with $Mesp1^{Cre}$ is embryonic lethal at E10.5 and mutants exhibit severely hypoplastic hearts.

Mef2cAHF::Cre is expressed from E7.5 onwards in anterior heart field (AHF) precursors, which contributes to the right ventricle and outflow tract; deletion of *Kmt2d* with *Mef2cAHF::Cre* is embryonic lethal at E13.5 and mutants exhibit defects in the outflow tract and interventricular septation.

Tnnt2::Cre is expressed from E7.5 onwards in the myocardium; deletion of *Kmt2d* with *Tnnt2::Cre* is embryonic lethal at E14.5 and mutants exhibit defects in interventricular septation.

(C) Immunostaining shows KMT2D expression is decreased in the nuclei of GFP-positive cells of AHF deletion mutant compared to control.

(D) Representative image showing control and $Mesp1^{Cre};Kmt2d^{fl/fl}$ mutant at E10.5. Mutant embryos exhibit severe developmental delay and pericardial edema compared to control littermates.

(E) Representative image showing control and $Mesp1^{Cre};Kmt2d^{fl/fl}$ mutant hearts at E10.5. Mutant hearts are severely hypoplastic compared to control littermates.

(F) Representative image showing H&E sections of control and *Mef2cAHF::Cre;Kmt2d* $^{fl/fl}$ mutant at E12.5. Mutant hearts exhibit disorganized myocardium, especially in the interventricular septum, compared to control littermates.

(G) Representative image showing control and *Mef2cAHF::Cre;Kmt2d* $^{fl/fl}$ mutant hearts at E12.5, with GFP reporter expressed in Cre-positive cells. Control littermates exhibit normal septation of outflow tract into the aorta and pulmonary artery, whereas mutants exhibit an unseptated outflow tract.

(H) Representative image showing H&E sections of control and *Tnnt2::Cre;Kmt2d* $^{fl/fl}$ mutant hearts at E13.5. Mutant hearts exhibit disorganized myocardium, especially in the interventricular septum, compared to control littermates.

(I) Cell cycle analysis by EdU labeling and flow cytometry of Cre-positive cells in E12.5 embryonic hearts revealed a significant decrease in the percentage of cells in G2/M phase in *Tnnt2::Cre;Kmt2d* $^{fl/fl}$ mutants compared to control littermates, indicating *Kmt2d* deletion led to cell cycle arrest in the G1/S phases.

(RA: Right atria; LA: Left atria; RV: Right ventricle; LV: Left ventricle; PA: pulmonary artery; OFT: outflow tract; IVS: interventricular septum)

Figure 3. Deletion of *Kmt2d* in cardiac precursors and myocardium lead to downregulation of ion transport related genes.

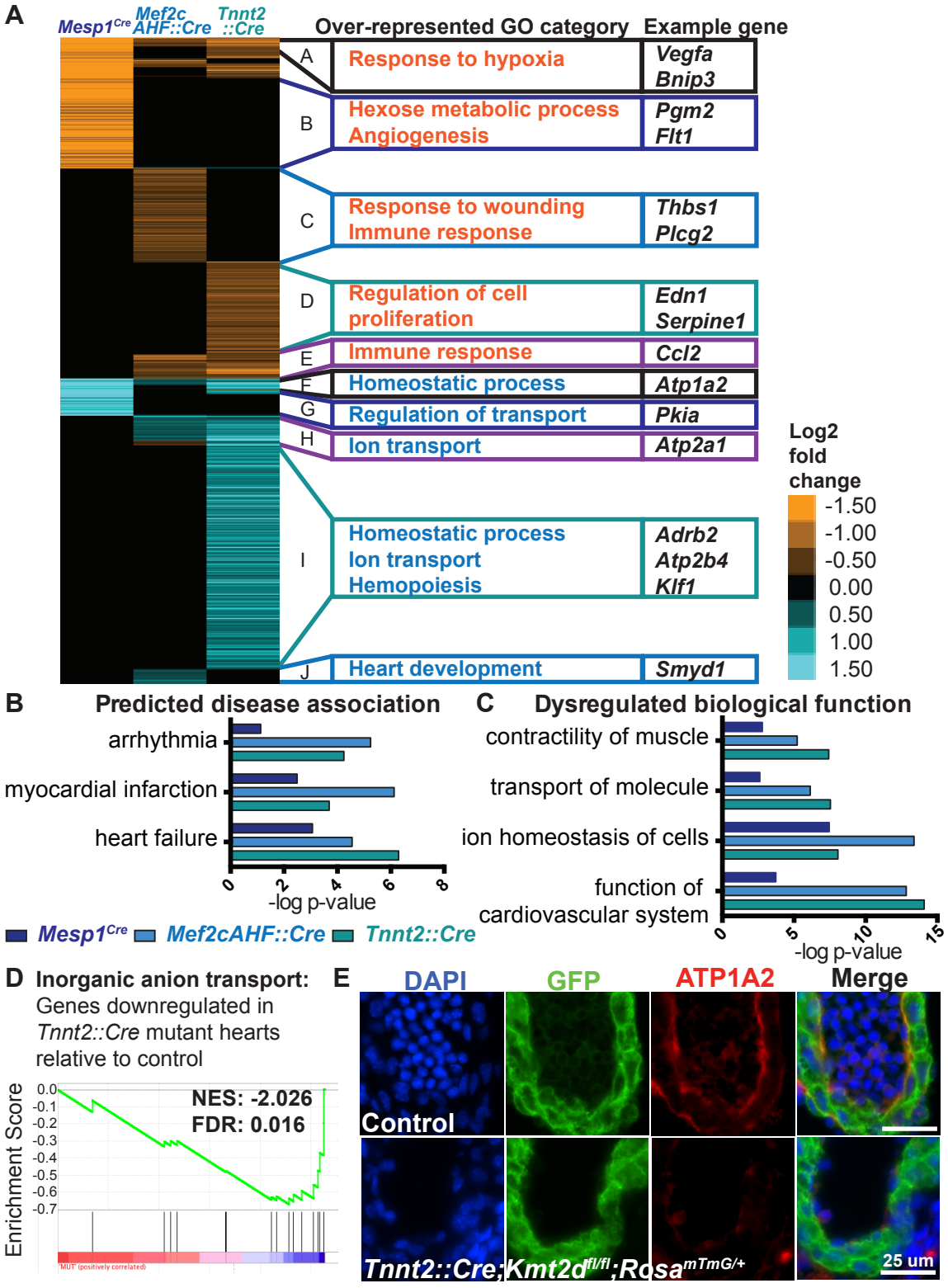

Figure 3. Deletion of *Kmt2d* in cardiac precursors and myocardium lead to downregulation of ion transport related genes.

(A) RNA-Seq analysis comparing differentially expressed genes in E9.0 *Mesp1*^{Cre}*; Kmt2d*$^{fl/fl}$ mutant hearts (FDR<0.01), E11.5 *Mef2cAHF::Cre;Kmt2d*$^{fl/fl}$ mutant hearts (FDR<0.05) and *Tnnt2::Cre;Kmt2d*$^{fl/fl}$ mutant hearts (FDR<0.05). Each genotype has distinct clusters of differentially expressed genes, indicating *Kmt2d* regulates different subsets of genes in each cardiac population. DAVID Gene Ontology analysis indicates an over-representation of hypoxia response genes in upregulated genes and an over-representation of ion transport related genes in downregulated genes.

(B) Ingenuity Pathway Analysis shows that biological functions that were significantly dysregulated in all three deletion mutants are associated with ion transport and cardiovascular function.

(C) Ingenuity Pathway Analysis shows that disease associations that were significantly predicted with all three deletion mutants are related to heart failure.

(D) GSEA shows a significant depletion of genes associated with inorganic anion transport in *Tnnt2::Cre;Kmt2d*$^{fl/fl}$ mutants.

(E) Immunostaining of E11.5 left atria shows decreased ATP1A2 expression in GFP positive cells in *Tnnt2::Cre;Kmt2d*$^{fl/fl}$ mutants, indicating the loss of ATP1A2 in Cre positive myocardial cells.

Figure 4. Myocardial deletion of *Kmt2d* results in a decrease in H3K4me2 levels at genes associated with ion transport.

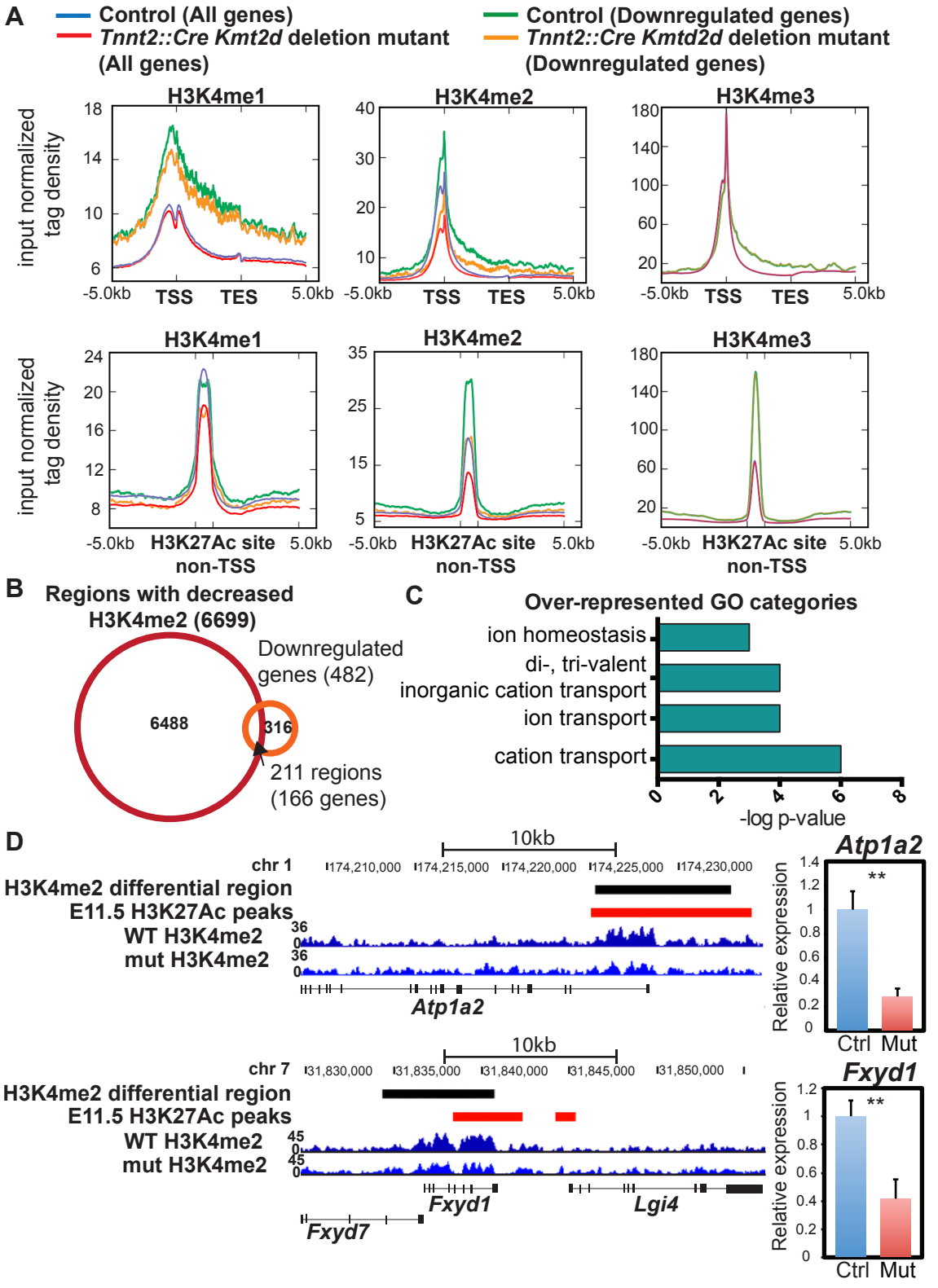

Figure 4. Myocardial deletion of *Kmt2d* results in a decrease in H3K4me2 levels at genes associated with ion transport.

(A) Metagene profiles showing the average distribution of H3K4me1, H3K4me2 and H3K4me3 at TSS and non-TSS H3K27Ac bound sites in E11.5 control and *Tnnt2::Cre;Kmt2d*$^{fl/fl}$ mutant hearts. Analysis of all genes and genes downregulated in mutants indicate a marked decrease in H3K4me2 levels in mutants at TSS and at non-TSS H3K27AC bound sites for all genes, with less noticeable effects on H3K4me1 and H3K4me3 levels. The same trend was observed at all downregulated genes from RNA-Seq dataset, although higher overall H3K4 methylation levels were observed at these genes in the control.

(B) 211 out of 6699 regions with decreased H3K4me2 levels corresponded with 166 downregulated genes in RNA-Seq of *Tnnt2::Cre;Kmt2d*$^{fl/fl}$ mutants.

(C) DAVID Gene Ontology analysis of 166 genes with decreased H3K4me2 levels and transcript levels indicates an over-representation of genes associated with ion transport.

(D) Ion transport related genes, such as *Atp1a2* and *Fxyd1*, exhibit a decrease in transcript levels and a decrease in H3K4me2 levels at the TSS and throughout the gene body.

(TSS: Transcription start site; TES: Transcription end site; WT: wild-type littermate controls; Mut: *Tnnt2::Cre;Kmt2d*$^{fl/fl}$ mutants)

Figure S1. *Kmt2d*$^{\Delta/+}$ mice have normal cardiac morphology and function.

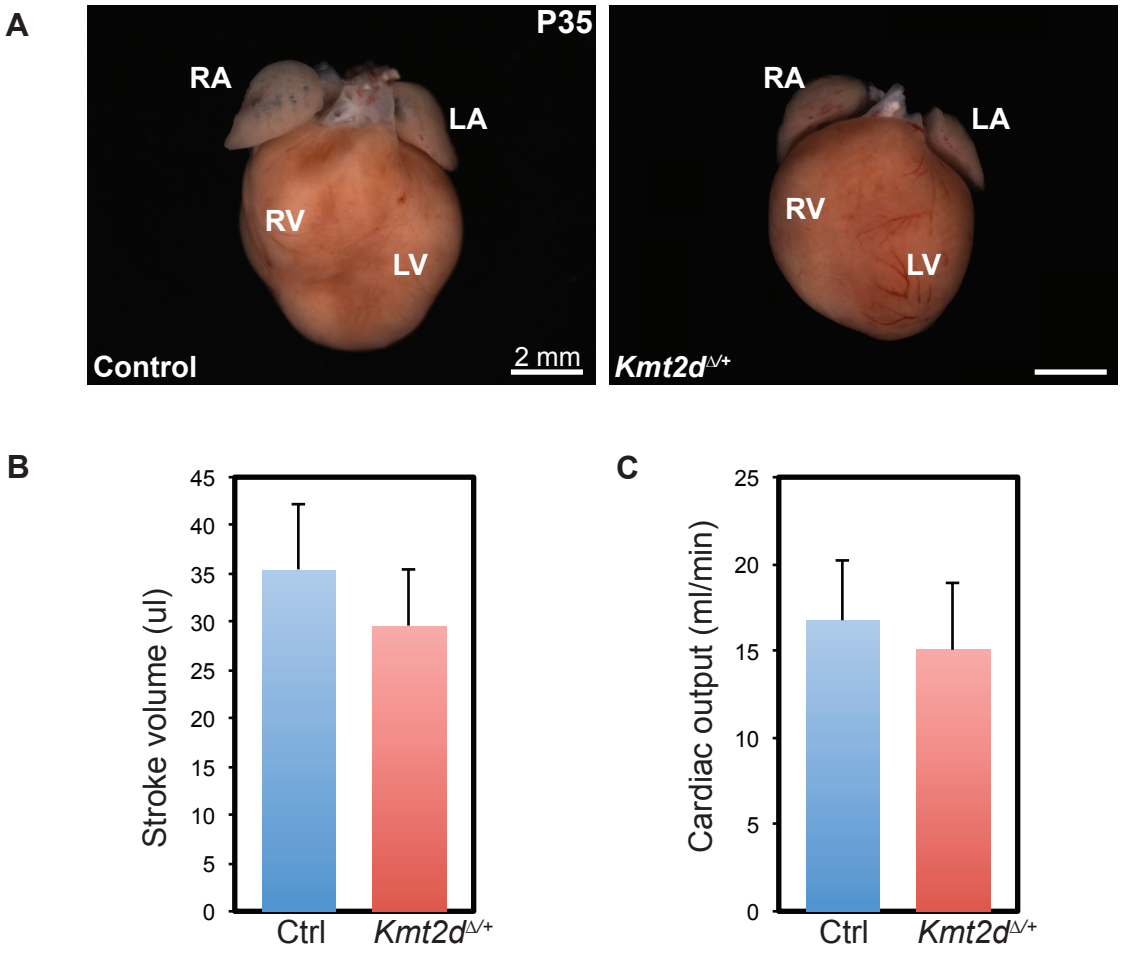

Figure S1. *Kmt2d*$^{\Delta/+}$ mice have normal cardiac morphology and function.

(A) *Kmt2d*$^{\Delta/+}$ and control hearts showed no differences in gross cardiac morphology.

(B) Stroke volume of P35 *Kmt2d*$^{\Delta/+}$ mutants do not show significant changes compared to control littermates.

(C) Cardiac output of P35 *Kmt2d*$^{\Delta/+}$ mutants do not show significant changes compared to control littermates.

(RA: Right atria; LA: Left atria; RV: Right ventricle; LV: Left ventricle)

Figure S2. Deletion of *Kmt2d* in cardiac precursors and myocardium leads to decrease in *Kmt2d* transcript and minor changes in gross morphology.

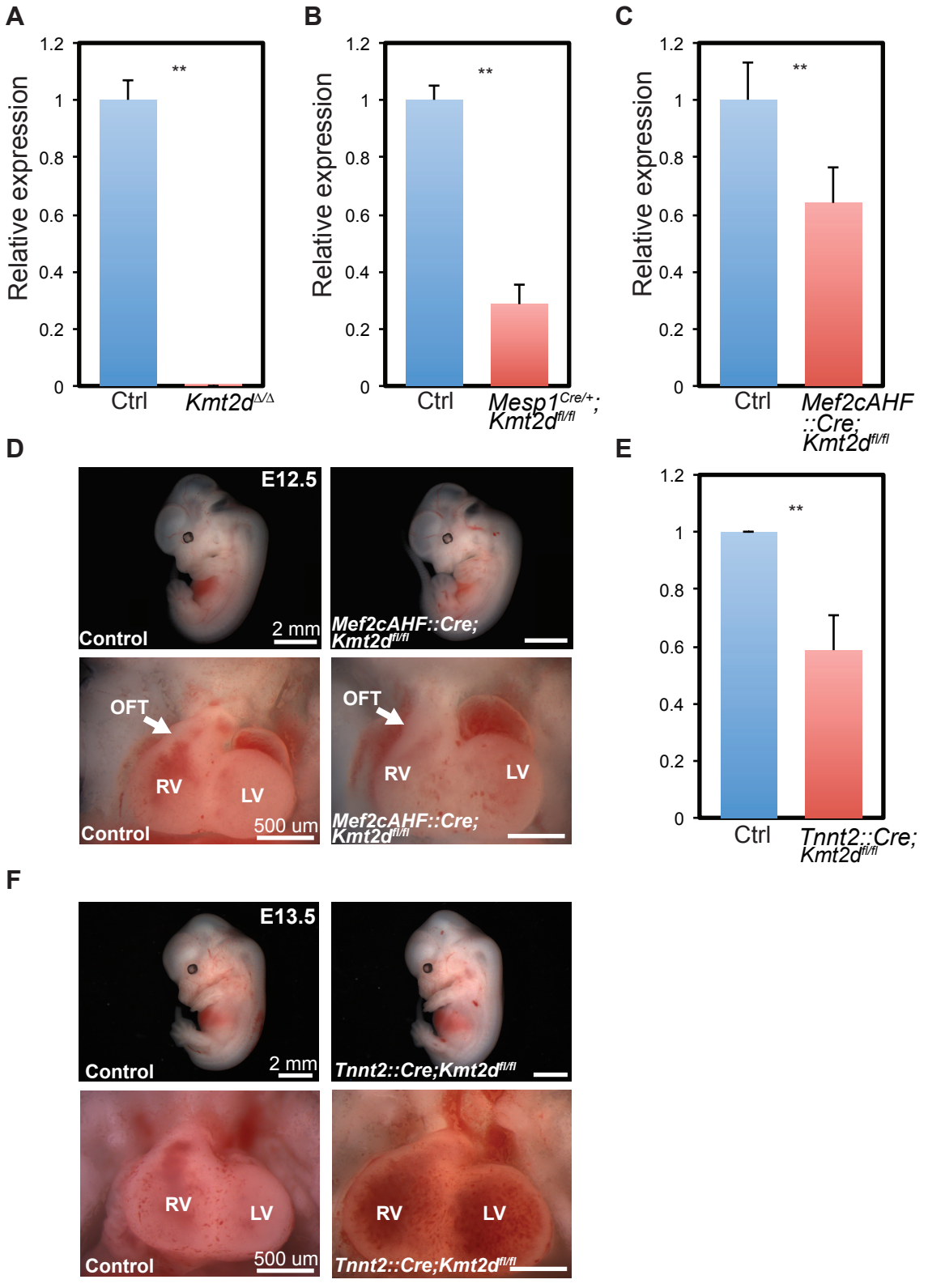

Figure S2. Deletion of *Kmt2d* in cardiac precursors and myocardium leads to decrease in *Kmt2d* transcript and minor changes in gross morphology.

(A) qRT-PCR of *Kmt2d* transcript levels show more than 95% decrease in E8.0 $Kmt2d^{\Delta/\Delta}$ mutants compared to control littermates.

(B) qRT-PCR of *Kmt2d* transcript levels show more than 70% decrease in E9.0 $Mesp1^{Cre};Kmt2d^{fl/fl}$ mutant hearts compared to control littermates.

(C) qRT-PCR of *Kmt2d* transcript levels show more than 35% decrease in E11.5 $Mef2cAHF::Cre;Kmt2d^{fl/fl}$ mutant hearts compared to control littermates.

(D) Representative image showing control and $Mef2cAHF::Cre;Kmt2d^{fl/fl}$ mutant embryos and hearts at E12.5. Mutants show similar gross morphology to littermates, but appear slightly paler and a shorter outflow tract is observed.

(E) qRT-PCR of *Kmt2d* transcript levels show more than 40% decrease in E11.5 $Tnnt2::Cre;Kmt2d^{fl/fl}$ mutant hearts compared to control littermates.

(F) Representative image showing control and $Tnnt2::Cre;Kmt2d^{fl/fl}$ mutant embryos and hearts at E13.5. Mutants show similar gross morphology to littermates, but appear slightly paler.

(OFT: outflow tract; RV: Right ventricle; LV: Left ventricle)

Figure S3. Deletion of *Kmt2d* in cardiac precursors and myocardium led to upregulation of hypoxia response genes due to a non-cell autonomous effect.

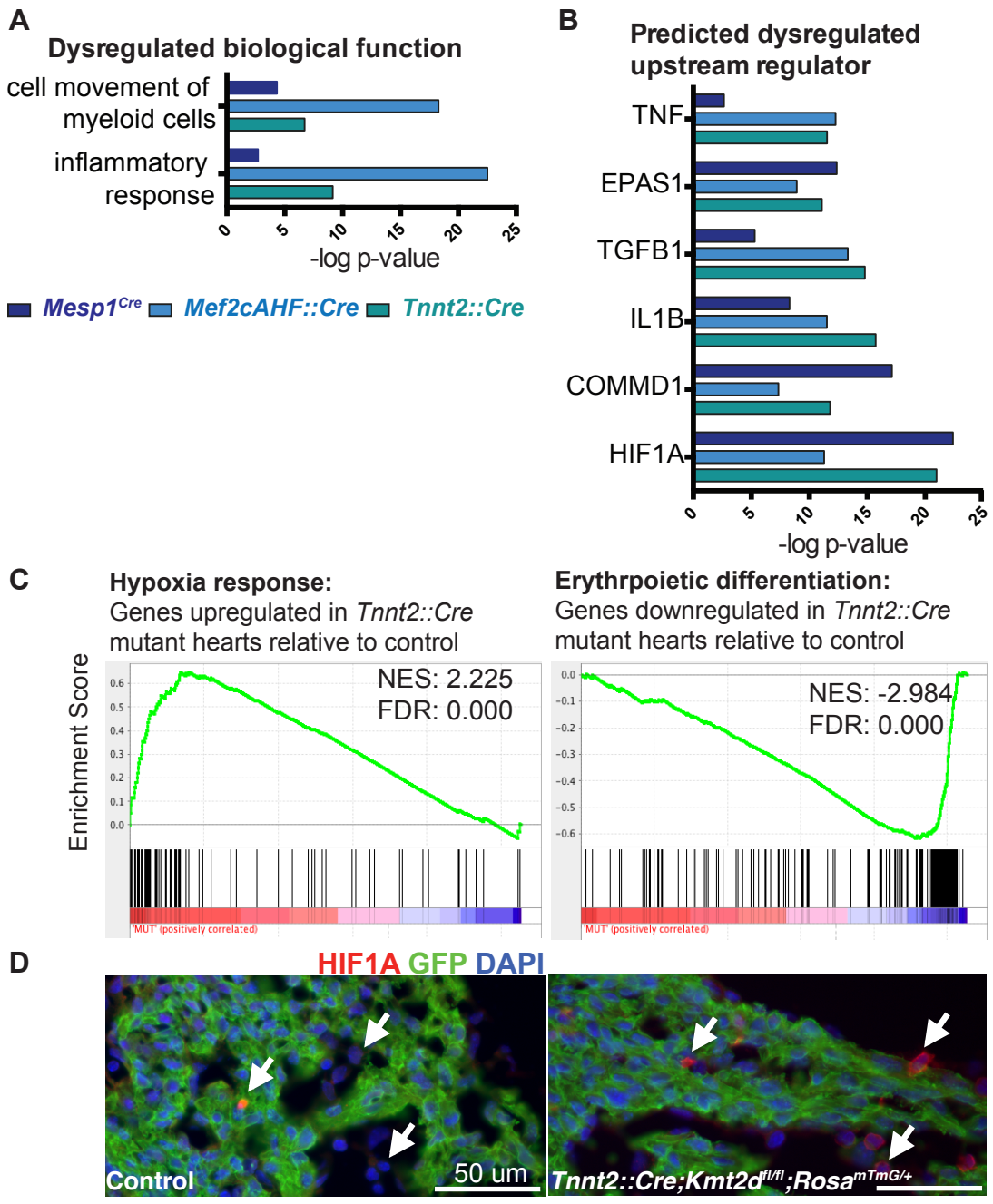

Figure S3. Deletion of *Kmt2d* in cardiac precursors and myocardium lead to upregulation of hypoxia response genes due to a non-cell autonomous effect.

(A) Ingenuity Pathway Analysis shows that biological functions that were significantly dysregulated in all three deletion mutants are associated with cell movement of myeloid cells and inflammatory response.

(B) Ingenuity Pathway Analysis shows that upstream regulators that were significantly predicted to be dysregulated in all three deletion mutants are associated with hypoxia.

(C) GSEA shows a significant enrichment of genes associated with hypoxia response and a significant depletion of genes associated with erythropoietic differentiation in *Tnnt2::Cre;Kmt2d*$^{fl/fl}$ mutants.

(D) Immunostaining of E11.5 interventricular septum shows increased HIF1A expression in GFP negative cells in *Tnnt2::Cre;Kmt2d*$^{fl/fl}$ mutants, indicating HIF1A is upregulated in Cre negative cells and the hypoxia response is due to a non-cell autonomous effect.

Figure S4. Myocardial deletion of *Kmt2d* results in a decrease in H3K4me2 levels at proximal and distal regulatory elements.

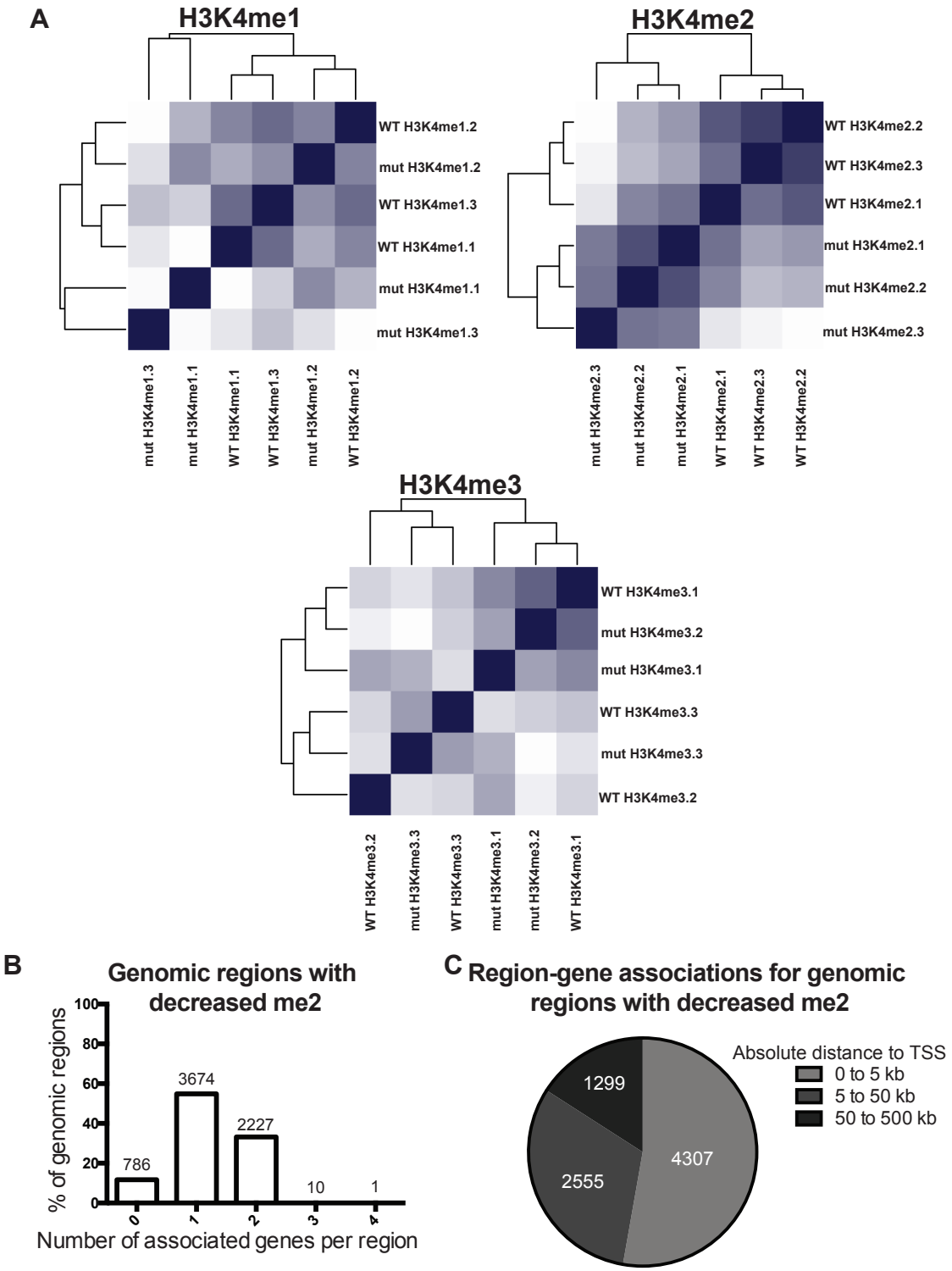

Figure S4. Myocardial deletion of *Kmt2d* results in a decrease in H3K4me2 levels at proximal and distal regulatory elements.

(A) Clustering analysis of ChIP-Seq peaks revealed that H3K4me2 peaks clustered tightly into control and mutant groups, whereas H3K4me1 and H3K4me3 peaks did not.

(B) GREAT analysis of the 6699 regions with decreased H3K4me2 associated 54.84% of the differential regions with 1 gene and 33.24% with 2 genes. 11.73% of the regions were not associated with any genes.

(C) GREAT analysis of decreased H3K4me2 region-gene associations revealed that that 52.72% of were located in within 5 kb of the TSS, whereas 31.28% were between 5 to 50 kb from the TSS, and 15.90% were found between 50 to 500kb from the TSS.

(TSS: Transcription Start Site)

Figure S5. Myocardial deletion of *Kmt2d* results in a decrease in H3K4me1 levels at genes associated with ion transport.

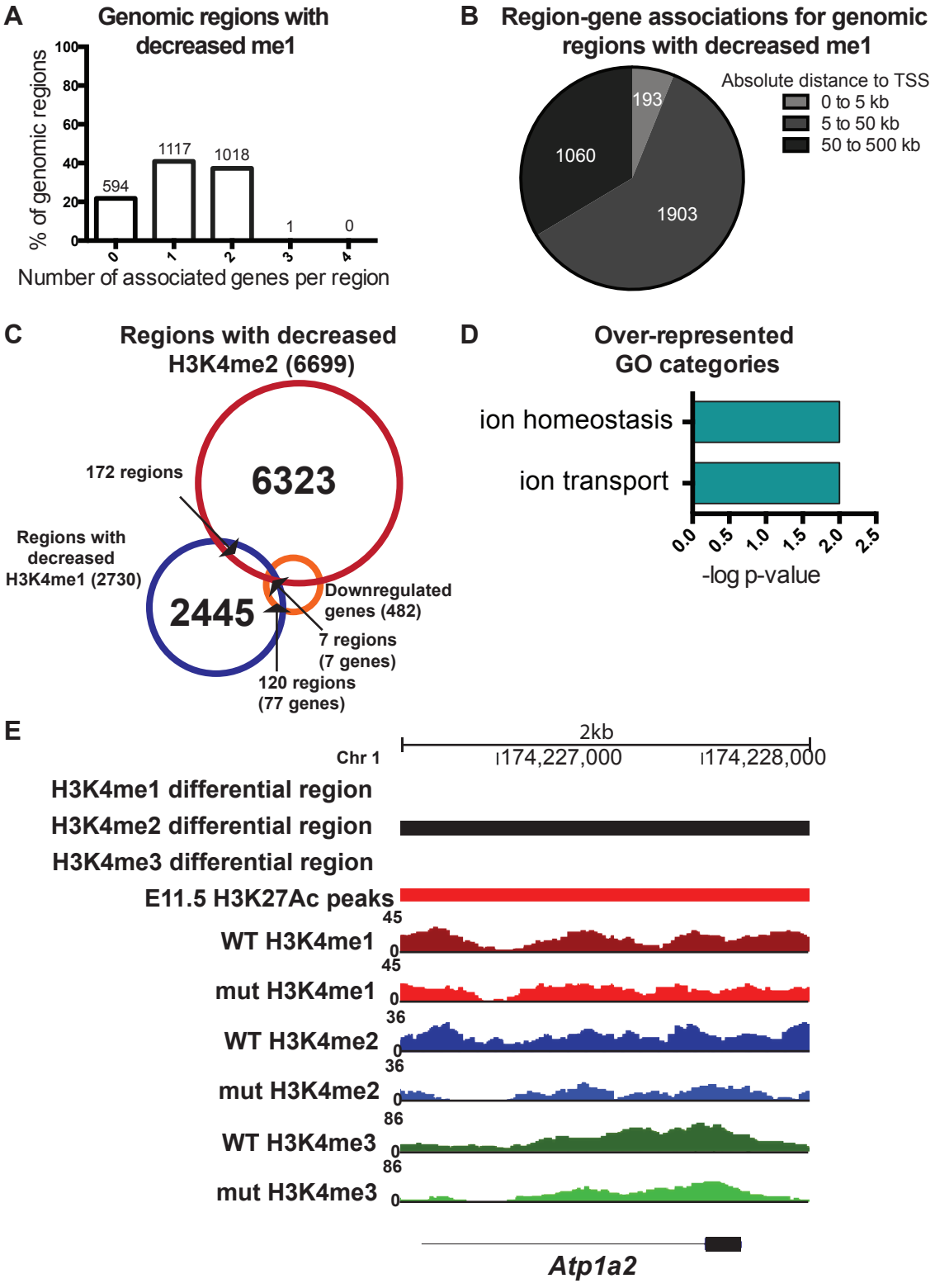

Figure S5. Myocardial deletion of *Kmt2d* results in a decrease in H3K4me1 levels at genes associated with ion transport.

(A) GREAT analysis of the 2730 regions with decreased H3K4me1 associated 40.92% of the differential regions with 1 gene and 37.29% with 2 genes. 21.76% of the regions were not associated with any genes.

(B) GREAT analysis of decreased H3K4me1 region-gene associations revealed that 6.11% were located in within 5 kb of the TSS, whereas 60.29% were between 5 to 50kb from the TSS, and 33.59% were found between 50 to 500kb from the TSS.

(C) Although 120 out of 2730 regions with decreased H3K4me1 corresponded with 77 downregulated genes from myocardial deletion mutant RNA-Seq data, there are only 172 regions with both decreased levels of H3K4me1 and H3K4me2, and only 7 of these regions corresponded to 7 downregulated genes.

(D) DAVID Gene Ontology analysis of 77 genes with decreased H3K4me1 and transcript levels indicates an over-representation of genes associated with ion homeostasis and transport.

(E) At the TSS of *Atp1a2*, there is a significant decrease in H3K4me2 levels, but no significant decrease in H3K4me1 and H3K4me3 levels.

(TSS: Transcription start site; WT: wild-type littermate controls; Mut: *Tnnt2::Cre;Kmt2d*$^{fl/fl}$ mutants)

Table 1. Genotypes of offspring obtained from *Kmt2d* deletion using *ACTB::Cre, Mesp1^{Cre}, Mef2cAHF::Cre* or *Tnnt2::Cre*.

Deletion in tissue	Stage	Total animals	Mutants	% mutants
Global (*ACTB::Cre*)	E8.0	31	8	25.81
	E8.5	9	0	0
	E9.5	26	0	0
	P0	21	0	0
Mesodermal precursors (*Mesp1^{Cre}*)	E8.5	12	2	16.67
	E9.0	17	4	23.53
	E9.5	38	7	18.42
	E10.5	15	0	0
	E11.5	8	0	0
	E12.5	5	0	0
	P0	45	0	0
Anterior heart field precursors (*Mef2cAHF::Cre*)	E9.5	14	4	28.57
	E10.5	96	21	21.88
	E11.5	40	8	20.00
	E12.5	39	7	17.95
	E13.5	14	0	0
	P0	96	0	0
Myocardium (*Tnnt2::Cre*)	E10.5	55	17	30.91
	E11.5	414	104	25.12
	E12.5	31	8	25.81
	E13.5	19	5	26.32
	E14.5	18	0	0
	E16.5	6	0	0
	P0	55	0	0

Chapter 3

Materials and Methods

Materials and Methods

Mice

Kmt2d$^{fl/fl}$ (referred to as *Mll4*$^{fl/fl}$ in Lee at al., 2014), *ACTB::Cre* (Lewandoski et al., 1997), *Mesp1*^{Cre} (Saga et al., 1999), *Mef2cAHF::Cre* (Verzi et al., 2005), *Rosa*^{mTmG} (Muzumdar et al., 2007), *Tnnt2::Cre* (Jiao et al., 2003) mice have been previously described. These mice were all backcrossed for at least five generations to a C57/BL6 background. Animals were housed and treated in accordance with the guidelines of the University of California, San Francisco (UCSF) Institutional Animal Care and Use Committee (IACUC). Conceptuses were generated from timed matings and detection of the vaginal plug was considered as embryonic day (E) 0.5.

Echocardiography

Echocardiograms to assess systolic function were performed using M-mode and 2-dimensional measurements as described previously (Garner et al., 2003). The measurements were made from five heterozygous *Kmt2d*$^{\Delta/+}$ mutants and five control littermates (n=5). The measurements represented the average of 6 selected cardiac cycles from at least 2 separate scans performed in random-blind fashion with papillary muscles as a point of reference for consistency in level of scan. End diastole was defined as the maximal left ventricular (LV) diastolic dimension, and end systole was defined as the peak of posterior wall motion. Fractional shortening (FS), a surrogate of systolic function, was calculated from

left ventricle dimensions as follows: FS=EDD−ESD/EDD×100%, where EDD is end-diastolic dimension and ESD is end-systolic dimension. Ejection fraction (EF) was calculated from 2-dimensional images.

Immunofluorescence

Trunk regions of embryos were dissected out and fixed in 4% paraformaldehyde for 30 minutes, followed by serial incubations in 10%, 20% and 30% sucrose and frozen in Tissue-Tek OCT Compound (Sakura Finetek, 4583). 8 um cryosections were obtained (Shandon Finesse 325 Manual Microtome) and mounted on glass slides. Cryosections were dried for 20 minutes at room temperature, washed with PBST (PBS with 0.3% Triton X-100) and incubated in blocking buffer (0.1M Tris HCl, pH 7.5, 0.15M NaCl, 0.5% PerkinElmer FP1012 blocking reagent) for 1 hour. Primary antibodies incubation was at 4˚C overnight in blocking buffer. Slides were washed with PBST and incubated with secondary antibodies for 1 hour, washed, stained with 1 ug/ul DAPI and mounted in Prolong Gold Antifade Mountant (P36930). Images were captured on a Leica DM5000 Microscope and compiled using ImageJ software (NIH; Bethesda, MD). Antibodies used are listed in Table S1.

Whole mount immunostaining

E12.5 embryonic hearts were dissected out and fixed in 4% paraformaldehyde for 3 hours, washed in PBT (PBS with 0.1% Tween), and incubated in blocking solution (5% serum, PBS, 0.5% Triton X-100) for 2 hours. Primary antibodies

incubation was at 4˚C overnight in blocking solution. Hearts were washed with PBT and incubated with secondary antibodies at 4˚C overnight in blocking solution. Hearts were washed with PBT, fixed again in 4% paraformaldehyde for 2 hours, and then washed with PBT. Images were captured on Leica MZFLIII Microscope and antibodies used are listed in Table S1.

Cell cycle analysis

200 ul of 5 mg/ml EdU in PBS were injected per 8-week old female mouse. After 2 hours, E12.5 whole hearts were dissected and dissociated to single cells by treating with TrypLE Express (Life Technologies) for 3 min at 37˚C. Dissociated single cells were fixed and EdU detection was performed using Click-iT Pacific Blue Flow Cytometry Assay Kit (Life Technologies) following the manufacturer's protocol for flow cytometry. Cells were stained with 7-AAD (7-Aminoactinomycin D, Life Technologies) for 30 minutes and analyzed on a LSR II (BD Biosciences). Data was analyzed using FlowJo software (Tree Star).

RNA Isolation and Quantitative PCR

Total RNA was isolated from embryonic hearts using RNAqueous Micro Total RNA Isolation Kit (Ambion). cDNA was generated using High Capacity cDNA Reverse Transcriptase Kit (Applied Biosystems) and qRT-PCR reactions were performed in triplicates using the Power SYBR Green Master Mix (Applied Biosystems) and ran on a 7900HT Real-Time PCR system (Applied Biosystems).

Relative abundance of mRNAs were calculated by normalization to *Actb* mRNA levels. Primer sequences are listed in Table S2.

RNA-Seq analysis

Whole genome gene expression analysis was performed on RNA isolated from control and mutant embryonic hearts. Libraries were prepared using Illumina TruSeq Paired-End Cluster Kit v3, and sequenced with the Illumina HiSeq 2500 system for pair-ended 100 base pairs (PE 100 bp). Reads were aligned to the reference assembly NCBI37/ mm9 (mouse) and assigned to genes using FeatureCounts (Liao et al., 2014). Differential expression was calculated either using edgeR (Robinson et al., 2011) or USeq (Nix et al., 2008). Differentially expressed genes were filtered with thresholds of FDR<0.05 or FDR<0.1, clustered using Cluster 3.0 and visualized with Treeview (Eisen et al., 1998). Gene ontology analysis was conducted using DAVID (Huang et al., 2009). RNA-Seq datasets were analyzed and functional analyses were generated through the use of QIAGEN's Ingenuity* Pathway Analysis (IPA) (IPA*, QIAGEN Redwood City, www.qiagen.com/ingenuity). Gene set enrichment analysis (GSEA) was performed as described (Subramanian et al., 2005).

Chromatin immunoprecipitation (ChIP)

90 *Tnnt2::Cre;Kmt2d*$^{fl/fl}$ hearts and 90 control hearts (from littermates) were collected at embryonic day 11.5. Formaldehyde was added to a final concentration of 1% to generate DNA-protein crosslinks for 10 minutes at room

temperature, then quenched by adding glycine to a final concentration of 125mM. Hearts were pelleted at 430g at 4C for 5 minutes and washed twice in 10mL of ice-cold PBS. Hearts were then resuspended in 3mL of ice-cold cell lysis buffer (5mM PIPES, pH 8.0; 85mM KCl; 1.0% (v/v) NP- 40; 1x protease inhibitor cocktail) and incubated on ice for 15 minutes. Next, hearts were homogenized on ice using a Dounce tissue grinder (20 strokes). Homogenate was pelleted at 430g at 4C for 5 minutes, then resuspended in ice-cold nuclei lysis buffer (50mM Tris-Cl, pH 8.0; 10mM EDTA, pH 8.0; 1% (w/v) SDS; 1x protease inhibitor cocktail). Samples were incubated in nuclei lysis buffer for 30 minutes on ice and sonicated using a Bioruptor Standard (Diagenode) (6x5min cycles, 30s on/30s off, 4C) to shear chromatin into 200- 600bp fragments. Samples were pelleted for 10 minutes at 20,800xg at 4C and supernatants were diluted 1:5 with IP dilution buffer (50mM Tris-Cl, pH 7.4; 150mM NaCl, 1mM EDTA, pH 8.0; 1% (v/v) NP-40; 0.25% (w/v) sodium deoxycholate; 1x protease inhibitor cocktail). 3ug of anti-H3K4me1 antibody, 3ug of anti-H3K4me2 antibody, or 3ug of anti-H3K4me3 antibody (listed in Table S1) were added to 3 control samples and 3 mutant samples (3 biological replicates per genotype per antibody). Samples were incubated overnight at 4˚C.

40uL of Protein G Dynabead (Life Technologies) suspension was added to each sample, incubated for 2 hours, then washed twice with IP wash buffer 1 (IP dilution buffer without protease inhibitors), twice with IP wash buffer 2 (100mM Tris-Cl, pH 9.0; 500mM LiCl; 1% (v/v) NP-40; 1% (w/v) sodium deoxycholate),

and with IP wash buffer 3 (100mM Tris-Cl, pH 9.0; 500mM LiCl; 150mM NaCl; 1% (v/v) NP-40; 1% (w/v) sodium deoxycholate). Immunoprecipitated material was eluted by incubating at 65C for 30 minutes with shaking in 100uL of ChIP elution buffer (50mM NaHCO3, 1% (w/v) SDS). NaCl was added to each eluted sample to a final concentration of 0.54M, and crosslinks were reversed by overnight incubation at 67˚C. Samples were treated with 10ug of RNase A for 30 minutes at 37˚C, and DNA was precipitated from each sample by adding 1.8x the sample volume of AMPure XP magnetic bead suspension (Beckman Coulter). Beads were washed 2x with 80% ethanol, dried, and beads were resuspended in 20uL water to elute DNA. Prepared libraries (Kapa Biosystems) were sequenced in 1x50bp mode on HiSeq 2500.

ChIP-Seq analysis

Reads are trimmed using the Fastq-mcf program. The filtered reads are analyzed using the FastQC program for quality control. Reads were aligned to the reference assembly NCBI37/ mm9 (mouse) using bowtie2, and Samtools is used to keep only the reads that do not map uniquely to the genome (mapq score >= 30). For tag calling, bam2bed is used to convert bam files into bed files, and the genome-wide shift between + and - strand tags is calculated in a manner adapted from the Kundaje method (Landt e al., 2012). For tag density calculation, the genome is divided into 20bp bins and tag density is defined as the number of tags that map to within 75bp of each genomic bin, followed by normalization over input tag density. To minimize false positives, bins representing greater than 6-

fold enrichment over background are accepted. Enriched bins are merged together throughout the genome and merged bins representing signal peaks spanning multiple genomic bins are retained. To compare peak scores and perform differential enrichment, peaks are annotated with total tag density within peak regions (Paige et al., 2012). Tag densities are converted into BigWig files and custom browser tracks are generated in the UCSC genome browser. Genomic regions with decreased H3K4 methylation levels with FDR<0.1 were associated with genes using GREAT (Mclean et al., 2010), with gene regulatory domain defined as proximal for 5 kb upstream and 1 kb upstream, distal for up to 100 kb in both directions to the nearest gene's basal domain.

Statistical analyses

Data are reported as mean ± SE and calculated using GraphPad Prism 6 software (La Jolla, CA). Chi-square tests were used to test for statistical significance in litter sizes. Unpaired two-tailed t-tests were used when comparing between mutant and control groups, with significant levels of *p≤ 0.05; **p ≤ 0.01 used for all statistical analyses.

Hypergeometric tests were performed to determine whether genes with decreased expression were more likely to be correlated with genes with decreased H3K4 methylation. The universal gene set contained any gene with FPKM>0 in either control or *Tnnt2::Cre; Kmt2d*$^{fl/fl}$ mutants using RNA-Seq gene expression data (27,233 genes), and 482 of these genes were downregulated. For ChIP-Seq performed on the same genotypes, our analysis yielded genomic

coordinates for regions with decreased H3K4 methylation and we used GREAT analysis to obtain associated genes (Mclean et al., 2010), filtering out genes not within the universal set. We assessed the probability that if we randomly selected *x* genes from the universal set (where *x* is the number of genes associated with decreased H3K4 methylation), we would get *y* correlated associations (where *y* is the number of genes associated with decreased H3K4 methylation correlated with decreased gene expression). We used the following hypergeometric test parameters: universal set = 27,233, subset 1 = 482, subset 2 = *x*, overlap = *y*. For H3K4me1, *x* = 2190, *y* = 77, hypergeometric test p-value = 1.25×10^{-13}. For H3K4me2, *x* = 5971, *y* = 166, hypergeometric test p-value = 1.10×10^{-18}. For H3K4me3, *x* = 33, *y* = 5, hypergeometric test p-value = 1.03×10^{-4}.

Supplementary tables

S1. List of antibodies used in this study.

Antibody	Company	Catalog No.	Host Isotype	Clone	Conjugate
Anti-KMT2D	Sigma-Aldrich	HPA035977	Rabbit IgG	N.A.	N.A.
Anti-ATP1A2	Abcam	ab2871	Mouse IgG1	M7-PB-E9	N.A.
Anti-HIF1A	Abcam	ab1	Mouse IgG2b	H1alpha67	N.A.
Anti-GFP	Abcam	ab13970	Chicken IgY	N.A.	N.A.
Anti-TPM1	DSHB	N.A.	Mouse IgG1	CH-1	N.A.
Anti-PECAM-1	BD Pharmingen	55370	Rat IgG2a	N.A.	N.A.
Anti-H3K4me1	Diagenode	C15410194	Rabbit IgG	pAb-194-050	N.A.
Anti-H3K4me2	Abcam	ab32356	Rabbit IgG	Y47	N.A.
Anti-H3K4me3	Millipore	07-473	Rabbit IgG	N.A.	N.A.
Anti-Rabbit Secondary	Invitrogen	A-11037	Goat	N.A.	Alexa 594
Anti-Mouse Secondary	Invitrogen	A-11032	Goat	N.A.	Alexa 594
Anti-Rat Secondary	Invitrogen	A-11007	Goat	N.A.	Alexa 594
Anti-Chicken Secondary	Invitrogen	A-11039	Goat	N.A.	Alexa 488

S2. List of primers used in this study.

Gene	F/R	Sequence
Kmt2d floxed allele (genotyping)	F	ATTGCATCAGGCAAATCAGC
	R	GCAGAAGCCTGCTATGTCCA
Kmt2d null allele (genotyping)	F	GTTCACTCAGTGGGGCTGTG
	R	GCAGAAGCCTGCTATGTCCA
Kmt2d exon 16-17 (qPCR)	F	GACCTGCTAATCCAGTGTCG
	R	CTGCTCCACCTCATCCTCTG
Actb (qPCR)	F	GCTCTTTTCCAGCCTTCCTT
	R	TGGCATAGAGGTCTTTACGGA

References

Abela D, et al. (2010) The effect of drugs with ion channel-blocking activity on the early embryonic rat heart. *Birth Defects Res Part B - Dev Reprod Toxicol* 89(5):429–440.

Adam MP, Hudgins L (2005) Kabuki syndrome: A review. *Clin Genet* 67(3):209–219.

Allis CD, et al. (2007) New Nomenclature for Chromatin-Modifying Enzymes. *Cell* 131(4):633–636.

Banka S, et al. (2012) How genetically heterogeneous is Kabuki syndrome?: MLL2 testing in 116 patients, review and analyses of mutation and phenotypic spectrum. *Eur J Hum Genet* 20:381-388.

Bjornsson HT, et al. (2014) Histone deacetylase inhibition rescues structural and functional brain deficits in a mouse model of Kabuki syndrome. *Sci Transl Med* 6(256):256ra135.

Bögershausen N, Bruford E, Wollnik B (2013) Skirting the pitfalls: A clear-cut nomenclature for H3K4 methyltransferases. *Clin Genet* 83(3):212–214.

Bruneau BG (2002) Transcriptional regulation of vertebrate cardiac morphogenesis. *Circ Res* 90(5):509–519.

Bruneau BG (2008) The developmental genetics of congenital heart disease. *Nature* 451(7181):943–948.

Bruneau BG (2010) Chromatin remodeling in heart development. *Curr Opin Genet Dev* 20(5):505–511.

Buckingham M, Meilhac S, Zaffran S (2005) Building the mammalian heart from two sources of myocardial cells. *Nat Rev Genet* 6(11):826–835.

Chang C-P, Bruneau BG (2012) Epigenetics and Cardiovascular Development. *Annu Rev Physiol* 74(1):41–68.

Chauhan C, Zraly CB, Dingwall AK (2013) The Drosophila COMPASS-like Cmi-Trr coactivator complex regulates dpp/BMP signaling in pattern formation. *Dev Biol* 380(2):185–198.

Cho YW, et al. (2007) PTIP associates with MLL3- and MLL4-containing histone H3 lysine 4 methyltransferase complex. *J Biol Chem* 282(28):20395–20406.

Christoffels VM, et al. (2000) Chamber formation and morphogenesis in the developing mammalian heart. *Dev Biol* 223(2):266–278.

Clark KL, et al. (2006) Transcription factors and congenital heart defects. *Annu Rev Physiol* 68:97–121.

Creyghton MP, et al. (2010) Histone H3K27ac separates active from poised enhancers and predicts developmental state. *Proc Natl Acad Sci U S A* 107(50):21931–21936.

Danielsson BR, Danielsson C, Nilsson MF (2007) Embryonic cardiac arrhythmia and generation of reactive oxygen species: Common teratogenic mechanism for IKr blocking drugs. *Reprod Toxicol* 24(1):42–56.

Danielsson BR, Skold AC, Azarbayjani F (2001) Class III antiarrhythmics and phenytoin: teratogenicity due to embryonic cardiac dysrhythmia and reoxygenation damage. *Curr Pharm Des* 7(9):787–802.

Danielsson BR, Sköld AC, Johansson A, Dillner B, Blomgren B (2003) Teratogenicity by the hERG potassium channel blocking drug almokalant: Use of hypoxia marker gives evidence for a hypoxia-related mechanism mediated via embryonic arrhythmia. *Toxicol Appl Pharmacol* 193(2):168–176.

Digilio MC, et al. (2001) Congenital heart defects in Kabuki syndrome. *Am J Med Genet* 100(4):269-274.

Eisen MB, Spellman PT, Brown PO, Botstein D (1998) Cluster analysis and display of genome-wide expression patterns. *Proc Natl Acad Sci U S A* 95(25):14863–14868.

Eissenberg JC, Shilatifard A (2010) Histone H3 lysine 4 (H3K4) methylation in development and differentiation. *Dev Biol* 339(2):240–249.

FitzGerald KT, Diaz MO (1999) MLL2: A new mammalian member of the trx/MLL family of genes. *Genomics* 59(2):187–192.

Garner LB, et al. (2003) Macrophage migration inhibitory factor is a cardiac-derived myocardial depressant factor. *Am J Physiol Heart Circ Physiol* 285(6):H2500–H2509.

Gitler AD, Lu MM, Jiang YQ, Epstein JA, Gruber PJ (2003) Molecular Markers of Cardiac Endocardial Cushion Development. *Dev Dyn* 228(4):643–650.

Guo C, et al. (2013) KMT2D maintains neoplastic cell proliferation and global histone H3 lysine 4 monomethylation. *Oncotarget* 4(11):2144–53.

Hang CT, et al. (2010) Chromatin regulation by Brg1 underlies heart muscle development and disease. *Nature* 466(7302):62–67.

Hannibal MC, et al. (2011) Spectrum of MLL2 (ALR) mutations in 110 cases of Kabuki syndrome. *Am J Med Genet Part A* 155(7):1511–1516.

Harvey RP (2002) Patterning the vertebrate heart. *Nat Rev Genet* 3(7):544–556.

Herz HM, et al. (2012) Enhancer-associated H3K4 monomethylation by trithorax-related, the drosophila homolog of mammalian MLL3/MLL4. *Genes Dev* 26(23):2604–2620.

Huang DW, Sherman BT, Lempicki RA (2009) Systematic and integrative analysis of large gene lists using DAVID bioinformatics resources. *Nat Protoc* 4(1):44–57.

Jiang X, Rowitch DH, Soriano P, McMahon AP, Sucov HM (2000) Fate of the mammalian cardiac neural crest. *Development* 127(8):1607–1616.

Jiao K, et al. (2003) An essential role of Bmp4 in the atrioventricular septation of the mouse heart. *Genes Dev* 17(19):2362–2367.

Källén B, Olaussonb OP (2006) Antidepressant drugs during pregnancy and infant congenital heart defect. *Reprod Toxicol* 21(3):221-222.

Kelly RG, Brown NA, Buckingham ME (2001) The Arterial Pole of the Mouse Heart Forms from Fgf10-Expressing Cells in Pharyngeal Mesoderm. *Dev Cell* 1(3):435–440.

Kim T, Buratowski S (2009) Dimethylation of H3K4 by Set1 Recruits the Set3 Histone Deacetylase Complex to 5' Transcribed Regions. *Cell* 137(2):259–272.

Lauberth SM, et al. (2013) H3K4me3 interactions with TAF3 regulate preinitiation complex assembly and selective gene activation. *Cell* 152(5):1021–1036.

Lee JE, et al. (2013) H3K4 mono- And di-methyltransferase MLL4 is required for enhancer activation during cell differentiation. *Elife* 2013(2). doi:10.7554/eLife.01503.

Lewandoski M, Meyers EN, Martin GR (1997) Analysis of Fgf8 gene function in vertebrate development. *Cold Spring Harbor Symposia on Quantitative Biology*, pp 159–168.

Li Y, et al. (2011) A mutation screen in patients with Kabuki syndrome. *Hum Genet* 130(6):715–724.

Liao Y, Smyth GK, Shi W (2014) FeatureCounts: An efficient general purpose program for assigning sequence reads to genomic features. *Bioinformatics* 30(7):923–930.

Lickert H, et al. (2004) Baf60c is essential for function of BAF chromatin remodelling complexes in heart development. *Nature* 432(7013):107–112.

Lin C-J, Lin C-Y, Chen C-H, Zhou B, Chang C-P (2012) Partitioning the heart: mechanisms of cardiac septation and valve development. *Development* 139(18):3277–3299.

Lodi M, et al. (2010) Seizures and EEG pattern in Kabuki syndrome. *Brain Dev* 32(10):829–834.

Makrythanasis P, et al. (2013) MLL2 mutation detection in 86 patients with Kabuki syndrome: A genotype-phenotype study. *Clin Genet* 84(6):539–545.

Malm H, Artama M, Gissler M, Ritvanen A (2011) Selective serotonin reuptake inhibitors and risk for major congenital anomalies. *Obstet Gynecol* 118(1):111–120.

Matsumoto N, Niikawa N (2003) Kabuki make-up syndrome: a review. *Am J Med Genet C Semin Med Genet* 117C(1):57–65.

Matsumoto N, Niikawa N (2003) Kabuki make-up syndrome: a review. *Am J Med Genet C Semin Med Genet* 117C(1):57–65.

McLean CY, et al. (2010) GREAT improves functional interpretation of cis-regulatory regions. *Nat Biotechnol* 28(5):495–501.

Micale L, et al. (2011) Mutation spectrum of MLL2 in a cohort of Kabuki syndrome patients. *Orphanet J Rare Dis* 6:38.

Miyake N, et al. (2013) MLL2 and KDM6A mutations in patients with Kabuki syndrome. *Am J Med Genet Part A* 161(9):2234–2243.

Mjaatvedt CH, et al. (2001) The outflow tract of the heart is recruited from a novel heart-forming field. *Dev Biol* 238(1):97–109.

Moorman AFM, Christoffels VM (2003) Cardiac chamber formation: development, genes, and evolution. *Physiol Rev* 83(4):1223–1267.

Muzumdar MD, Tasic B, Miyamichi K, Li N, Luo L (2007) A global double-fluorescent cre reporter mouse. *Genesis* 45(9):593–605.

Ng SB, et al. (2010) Exome sequencing identifies MLL2 mutations as a cause of Kabuki syndrome. *Nat Genet* 42(9):790–793.

Nimura K, et al. (2009) A histone H3 lysine 36 trimethyltransferase links Nkx2-5 to Wolf-Hirschhorn syndrome. *Nature* 460(7252):287–291.

Nix DA, Courdy SJ, Boucher KM (2008) Empirical methods for controlling false positives and estimating confidence in ChIP-Seq peaks. *BMC Bioinformatics* 9:523.

Nord AS, et al. (2013) Rapid and pervasive changes in genome-wide enhancer usage during mammalian development. *Cell* 155(7):1521–1531.

Nührenberg T, Gilsbach R, Preissl S, Schnick T, Hein L (2014) Epigenetics in cardiac development, function, and disease. *Cell Tissue Res* 356(3):585–600.

Olson EN (2006) Gene regulatory networks in the evolution and development of the heart. *Science* 313(5795):1922–1927.

Park CY, et al. (2010) skNAC, a Smyd1-interacting transcription factor, is involved in cardiac development and skeletal muscle growth and regeneration. *Proc Natl Acad Sci U S A* 107(48):20750–20755.

Paulussen ADC, et al. (2011) MLL2 mutation spectrum in 45 patients with Kabuki syndrome. *Hum Mutat* 32(2). doi:10.1002/humu.21416.

Pedersen LH, Henriksen TB, Vestergaard M, Olsen J, Bech BH (2009) Selective serotonin reuptake inhibitors in pregnancy and congenital malformations: population based cohort study. *BMJ* 339(sep23 1):b3569–b3569.

Pekowska A, Benoukraf T, Ferrier P, Spicuglia S (2010) A unique H3K4me2 profile marks tissue-specific gene regulation. *Genome Res* 20(11):1493–1502.

Popova EY, et al. (2012) Stage and Gene Specific Signatures Defined by Histones H3K4me2 and H3K27me3 Accompany Mammalian Retina Maturation In Vivo. *PLoS One* 7(10). doi:10.1371/journal.pone.0046867.

Ream M, Ray AM, Chandra R, Chikaraishi DM (2008) Early fetal hypoxia leads to growth restriction and myocardial thinning. *Am J Physiol Regul Integr Comp Physiol* 295(2):R583–R595.

Restivo A, Piacentini G, Placidi S, Saffirio C, Marino B (2006) Cardiac outflow tract: A review of some embryogenetic aspects of the conotruncal region of the heart. *Anat Rec - Part A Discov Mol Cell Evol Biol* 288(9):936–943.

Robinson M, Mccarthy D, Chen Y, Smyth GK (2011) edgeR : differential expression analysis of digital gene expression data User ' s Guide. *Most* 23(July):1–77.

Ruthenburg AJ, Allis CD, Wysocka J (2007) Methylation of Lysine 4 on Histone H3: Intricacy of Writing and Reading a Single Epigenetic Mark. *Mol Cell* 25(1):15–30.

Saga Y, et al. (1999) MesP1 is expressed in the heart precursor cells and required for the formation of a single heart tube. *Development* 126(15):3437–3447.

Samsa LA, Yang B, Liu J (2013) Embryonic cardiac chamber maturation: Trabeculation, conduction, and cardiomyocyte proliferation. *Am J Med Genet Part C Semin Med Genet* 163(3):157–168.

Shah M, Bogucki B, Mavers M, deMello DE, Knutsen A (2005) Cardiac conduction abnormalities and congenital immunodeficiency in a child with Kabuki syndrome: case report. *BMC Med Genet* 6:28.

Shilatifard A (2012) The COMPASS Family of Histone H3K4 Methylases: Mechanisms of Regulation in Development and Disease Pathogenesis. *Annu Rev Biochem* 81(1):65–95.

Sims RJ, et al. (2002) m-Bop, a repressor protein essential for cardiogenesis, interacts with skNAC, a heart- and muscle-specific transcription factor. *J Biol Chem* 277(29):26524–26529.

Sköld AC, Danielsson C, Linder B, Danielsson BR (2002) Teratogenicity of the IKr-blocker cisapride: Relation to embryonic cardiac arrhythmia. *Reprod Toxicol* 16(4):333–342.

Sköld AC, Wellfelt K, Danielsson BR (2001) Stage-specific skeletal and visceral defects of the IKr-blocker almokalant: Further evidence for teratogenicity via a hypoxia-related mechanism. *Teratology* 64(6):292–300.

Stein AB, et al. (2011) Loss of H3K4 methylation destabilizes gene expression patterns and physiological functions in adult murine cardiomyocytes. *J Clin Invest* 121(7):2641–2650.

Subramanian A, et al. (2005) Gene set enrichment analysis: a knowledge-based approach for interpreting genome-wide expression profiles. *Proc Natl Acad Sci U S A* 102(43):15545–50.

Takeuchi JK, Bruneau BG (2009) Directed transdifferentiation of mouse mesoderm to heart tissue by defined factors. *Nature* 459(7247):708–711.

Takeuchi JK, et al. (2011) Chromatin remodelling complex dosage modulates transcription factor function in heart development. *Nat Commun* 2:187.

Van Der Linde D, et al. (2011) Birth prevalence of congenital heart disease worldwide: A systematic review and meta-analysis. *J Am Coll Cardiol* 58(21):2241–2247.

Van Weerd JH, Koshiba-Takeuchi K, Kwon C, Takeuchi JK (2011) Epigenetic factors and cardiac development. *Cardiovasc Res* 91(2):203–211.

Verrotti A, et al. (2011) Long-term outcome of epilepsy in Kabuki syndrome. *Seizure* 20(8):650–654.

Verzi MP, McCulley DJ, De Val S, Dodou E, Black BL (2005) The right ventricle, outflow tract, and ventricular septum comprise a restricted expression domain within the secondary/anterior heart field. *Dev Biol* 287(1):134–145.

Waldo KL, et al. (2001) Conotruncal myocardium arises from a secondary heart field. *Development* 128(16):3179–3188.

Wan X, et al. (2014) Mll2 Controls Cardiac Lineage Differentiation of Mouse Embryonic Stem Cells by Promoting H3K4me3 Deposition at Cardiac-Specific Genes. *Stem Cell Rev Reports*. doi:10.1007/s12015-014-9527-y.

Wang Z, et al. (2004) Polybromo protein BAF180 functions in mammalian cardiac chamber maturation. *Genes Dev* 18(24):3106–3116.

Webster WS, Brown-Woodman PDC, Snow MD, Danielsson BRG (1996) Teratogenic potential of almokalant, dofetilide, and d-sotalol: Drugs with potassium channel blocking activity. *Teratology* 53(3):168–175.

Wellfelt K, Sköld AC, Wallin A, Danielsson BR (1999) Teratogenicity of the class III antiarrhythmic drug almokalant. Role of hypoxia and reactive oxygen species. *Reprod Toxicol* 13(2):93–101.

Wong P, et al. (2011) Gene induction and repression during terminal erythropoiesis are mediated by distinct epigenetic changes. *Blood* 118(16). doi:10.1182/blood-2011-03-341404.

Wurst KE, Poole C, Ephross SA, Olshan AF (2010) First trimester paroxetine use and the prevalence of congenital, specifically cardiac, defects: A meta-analysis of epidemiological studies. *Birth Defects Res Part A - Clin Mol Teratol* 88(3):159–170.

Yin Z, et al. (2002) The essential role of Cited2, a negative regulator for HIF-1α, in heart development and neurulation. *Proc Natl Acad Sci U S A* 99(16):10488–10493.

Yoon JK, et al. (2015) The strong association of left-side heart anomalies with Kabuki syndrome. *Korean J Pediatr* 58(7):256-262.

Yuan SM (2013) Congenital heart defects in Kabuki syndrome. *Cardiol J* 20(2):121–124.

Zaidi S, et al. (2013) De novo mutations in histone-modifying genes in congenital heart disease. *Nature* 498(7453):220–3.

Publishing Agreement

It is the policy of the University to encourage the distribution of all theses, dissertations, and manuscripts. Copies of all UCSF theses, dissertations, and manuscripts will be routed to the library via the Graduate Division. The library will make all theses, dissertations, and manuscripts accessible to the public and will preserve these to the best of their abilities, in perpetuity.

I hereby grant permission to the Graduate Division of the University of California, San Francisco to release copies of my thesis, dissertation, or manuscript to the Campus Library to provide access and preservation, in whole or in part, in perpetuity.

Author Signature

September 3, 2015

Date